



1 **Geosystemics and Earthquakes**

2

3 Angelo De Santis^(1,2), Gianfranco Cianchini⁽¹⁾, Rita Di Giovambattista⁽¹⁾, Cristoforo Abbattista⁽³⁾,

4 Lucilla Alfonsi⁽¹⁾, Leonardo Amoruso⁽³⁾, Marianna Carbone⁽³⁾, Claudio Cesaroni⁽¹⁾, Giorgiana De

5 Franceschi⁽¹⁾, Anna De Santis⁽¹⁾, Alessandro Ippolito⁽¹⁾, Dedalo Marchetti⁽¹⁾, Luca Martino⁽²⁾,

6 Francisco Javier Pavòn-Carrasco^(1,4), Loredana Perrone⁽¹⁾, Alessandro Piscini⁽¹⁾, Mario Luigi

7 Rainone⁽²⁾, Luca Spogli^(1,5) and Francesca Santoro⁽³⁾

8

9

10 ⁽¹⁾ Istituto Nazionale di Geofisica e Vulcanologia – Sez. Roma 2, Rome (Italy)

11 ⁽²⁾ Università G. D’Annunzio, INGEO Department, Chieti (Italy)

12 ⁽³⁾ Planetek Italia srl, via Massaua 12, Bari (Italy)

13 ⁽⁴⁾ Now at Facultad Física (UCM), Avd. Complutense, s/n. 28040 – Madrid (Spain)

14 ⁽⁵⁾ SpacEarth Technology, Rome, Italy

15

16

17 **Abstract**

18

19 Geosystemics [De Santis 2009, 2014] studies the Earth system as a whole focusing on the possible
20 coupling among the Earth layers (the so called *geo-layers*), and using universal tools to integrate
21 different methods that can be applied to multi-parameter data, often taken on different platforms. Its
22 main objective is to understand the particular phenomenon of interest from a holistic point of view.

23 In this paper we will deal with earthquakes, considered as a long term chain of processes involving,
24 not only the interaction between different components of the Earth’s interior, but also the coupling
25 of the solid earth with the above neutral and ionized atmosphere, and finally culminating with the
26 main rupture along the fault of concern [De Santis et al., 2015a]. Some case studies (particular
27 emphasis is given to recent central Italy earthquakes) will be discussed in the frame of the
28 geosystemic approach for better understanding the physics of the underlying complex dynamical
29 system.

30

31

32

33



1 **1. Introduction**

2

3

4 The present times are difficult for humankind: although civilization, together with technology, has
5 reached its greatest level, the cost to pay is that modernization has simultaneously involved some
6 level of higher vulnerability than in the past (e.g. Nott, 2006). Humankind is affecting some parts of
7 Nature, but, unfortunately, without perfect control. Natural hazards, e.g. hurricanes, earthquakes
8 (EQs), floods, tsunamis, and other kinds of catastrophes, are often out of human control and the
9 consequences are unpredictable. They happen as extreme events on the planet causing destruction
10 and deaths (Meyers, 2009), and the occurrence of most of them looks as increasing dramatically in
11 the last century (Peduzzi, 2005). Present society, although reaching a high technological level, is
12 still very weak, and no strong remedy and rapid resilience are fully possible (Bunde et al., 2002).

13

14 There is no other solution than attempting to understand how our planet works and what possible
15 future sceneries are. To do this, we cannot limit our approach to a reductionist one, but we also need
16 to study the Earth as a whole system, where all parts are nonlinearly interconnected and useful for
17 the system to evolve (e.g. Skinner and Porter, 1995). In contrast with the reductionist approach, the
18 latter does not look at Earth as a precise clock system where all components have their distinct own
19 purpose (often called as the Laplacian point of view), rather we have to consider it as an ensemble
20 of cross-interacting parts put together in order to reach the same ambitious goal that, at the present
21 knowledge, seems to be rare in the Universe: to maintain life (Lovelock, 1972). Earth system is
22 both composed of living organisms and soft and hard engines, in a continuous balance and
23 competition between life and death, heat and cold, complexity and simplicity, chaos and non-chaos.

24

25 In this paper we will remind the concepts of Geosystemics and then apply it to EQs, through some
26 specific concepts such as the changes of Benioff strain, Entropy, temperature, etc., in the frame of a
27 Lithosphere-Atmosphere-Ionosphere (LAI) coupling model, i.e. some quantities that are related to
28 macroscopic features of the system under study.

29

30 Even if many efforts have been made towards a deeper knowledge of EQs, in terms of experimental,
31 theoretical and numerical models (e.g. Aki & Richard, 2002; Bizzarri, 2011, 2012), their evolution
32 phases are not exhaustively explained yet. A possible explanation of this uncertainty is the lack of
33 knowledge regarding the source initiation, the fracture mechanisms and dynamics of the crust (e.g.
34 Scholz, 2002). Moreover, each EQ initiates and develops in its proper geodynamical and



1 lithological settings, this giving an almost unique character to each event. Thus, to reach the
2 knowledge necessary to recognise in advance the eventual rupture (failure) of the fault which causes
3 the occurrence of the EQ is a greatly difficult task itself. Difficult as well is the possible explanation
4 of the various and often weak phenomena affecting the above atmosphere and ionosphere, where
5 even many external causes act to mix together signals which are different in spectral content and
6 amplitudes.

7

8 Despite all these difficulties, one of the most eminent seismologists, Hiroo Kanamori (1981),
9 pointed out that some common physical mechanisms beneath the generation processes may act,
10 although controlled by the local geodynamic forces and heterogeneities of the lithology (Baskoutas
11 and Papadopoulos, 2014): this thought encourages the efforts towards a deeper knowledge of the
12 physics behind such a complex phenomenon as the EQ.

13

14 If the process of rupture that causes the EQ is still plenty of open issues and unanswered questions
15 (e.g. Bizzarri, 2014), even more difficult is the understanding of the process of EQ preparation,
16 although some efforts have been performed (e.g. Dobrovolsky et al. 1979, 1989; Sobolev et al.
17 2002) as is thought to be accompanied by some exchanges of mass and energy, which can change
18 the energy budget in the earth-atmosphere system over the seismogenic zone and, in fact, scientific
19 literature reports a wide variety of phenomena preceding EQs which have been studied extensively
20 with the aim of finding some recurrent and recognizable patterns: induced electric and magnetic
21 fields, groundwater level changes, gas and infrared (IR) electromagnetic emissions, local
22 temperature changes, surface deformations (see Cicerone et al., 2009 and De Santis et al., 2015a for
23 more exhaustive reviews).

24

25 Being Geosystemics introduced by one of the present coauthors, great part of this paper is based on
26 own contributions from mostly already published material. However we attempted to give new
27 insights on the idea of Geosystemics with also some unpublished own material or other researchers'
28 contributions.

29

30 At first, we place the present view of Geosystemics and show the application to some case studies.
31 We also present a possible physical model that attempts to explain the found results. We then
32 conclude with some feasible future directions and conclusions.

33

34



1 2. Geosystemics

2

3

4 We depict here the general concepts of geosystemics in order to be then applied to EQs in the next
5 section.

6

7 Geosystemics looks at the Earth system in its whole: in particular, it focuses on self-regulation
8 phenomena and relations among the parts composing the Earth. Dynamically speaking, it also
9 searches for the possible trends of change or persistence of the specific system or sub-system under
10 study (De Santis, 2009, 2014, De Santis and Qamili, 2015). To perform this, geosystemics applies
11 mainly the concepts of entropy and information content to time series characterising the
12 phenomenon under study: to measure and understand the physical world, not only energy and
13 matter are important, but also information (Bekenstein, 2003). Interesting features of the complex
14 system under study to investigate are: nonlinear coupling and new emergent behaviour, self-
15 regulation, and irreversibility as important constituents of the Earth planet.

16

17 The most important basic concept of geosystemics is that no layer of the Earth system is really
18 isolate, rather it communicates (in terms of transfer of energy or particles) with the other ones. This
19 concept is more strengthened in case of very powerful phenomena that release a large energy in a
20 short time, such as the earthquakes in the lithosphere (for a M7 earthquake, around 10^{15} Joule are
21 released in some seconds), the lightning strikes in atmosphere (around 10^9 J in microseconds),
22 etcetera. For instance, the information exchanged between contiguous parts of the Earth system
23 producing increased entropy would allow us to better recognise and understand those irreversible
24 processes occurring in the Earth's interior. As said in De Santis and Qamili (2015), "*Geosystemics*
25 *has the objective to observe, study, represent and interpret those aspects of geophysics that*
26 *determine the structural characteristics and dynamics of our planet and the complex interactions of*
27 *the elements that compose it*" by means of some entropic measures.

28

29 Together with this, the approach will be based on multi-scale/parameter/platform observations in
30 order to better scrutinise the particular sub-systems of Earth under study as much as possible. This
31 is a fundamental issue of geosystemics, because there is no better way to understand the behaviour
32 of a complex system than looking at it from as many perspectives and points of view as possible.
33 Recent advanced examples to observe the planet are from satellites (e.g. Chuvieco and Huete, 2009)
34 and seafloors (Favali et al., 2015).



1 Geosystemics differs from the standard Earth System Science (e.g. Schneider and Boston, 1992;
2 Skinner and Porter 1995; Jacobson et al., 2000; Butz, 2004): for instance, in the way it is applied by
3 means of entropic measures to different physical quantities, this because entropy is the only entity
4 that can be used to have some clues on the next future (please remind the second law of
5 thermodynamics; e.g. Grandy, 2008).

6

7 In this paper, we will concentrate the attention to the application to EQ physics study and the
8 possibility for intermediate and/or short-term prediction. Here, with the term “prediction”, we mean
9 the possibility to make a prediction about EQ occurrence, magnitude and location, with small
10 uncertainty, i.e. in a deterministic way, in contrast with the probabilistic approach used in EQ
11 forecast (please see also in the next section for other details on this question). In particular, we will
12 explore the present state-of-the-art of the seismological diagnostic tools based on a macroscopic
13 point of view. Particular emphasis will be dedicated to the above mentioned Shannon entropy. Later
14 on, we also see another one that quantifies the sense of flow of information, the transfer entropy
15 (Schreiber, 2000).

16

17

18

19 **3. Main seismological diagnostic tools**

20

21

22 The Holy Grail in seismology is to reach the capability of giving short-term prediction of large EQs
23 thus eventually saving lives. Unfortunately, it is not an easy task as testified by the great all-out and
24 full scale effort made with this aim in many fields of research (even far from the traditional field of
25 seismology) and the corresponding huge amount of scientific papers claiming or denying success or
26 simply attempting some important steps forward towards the goal. However, despite of the many
27 attempts no significant success has been clearly counted (Hough, 2009).

28

29 Regarding the methods to make EQ “predictions”, we can classify them in (mainly) *deterministic*
30 and (mainly) *stochastic* methods. The bracket term “(mainly)” is placed because, actually, no
31 method is only deterministic or stochastic. To be operative, we can define the latter methods as
32 those that provide a forecast with some level of probability, for which the probability of no EQ is
33 always different than zero, while the deterministic methods attempt to indicate the approaching of a



1 large EQ with some level of confidence, i.e. with small uncertainty in space and time of occurrence,
2 and magnitude.

3

4 Several statistical methods have been applied in the last decades to seismological data (mainly
5 catalogs) with the aim of improving the knowledge on seismic phenomena. At present, the scientific
6 community is involved in global projects to test and evaluate the performances of some well
7 established algorithms in different tectonic environments (see <http://www.cseptesting.org/>;
8 <http://www.corssa.org/> websites). According to CSEP (Collaboratory for the Study of Earthquake
9 Predictability), the most important steps of an earthquake prediction protocol are the following
10 ones:

11

12 1. *Present a physical model that can explain the proposed precursor anomaly.*

13 2. *Exactly define the anomaly and describe how it can be observed.*

14 3. *Explain how a precursory information can be translated into a forecast and specify such a
15 forecast in terms of probabilities for given space/time/magnitude windows.*

16 4. *Perform a test over some time that allows to evaluate the proposed precursor and its forecasting
17 power.*

18 5. *Report on successful prediction, missed earthquakes, and false predictions.*

19

20 In this part, we will focus our attention to the deterministic methods, which are essentially based on
21 a systematic catalog-based search of some peculiar *seismicity pattern recognition* in the given area
22 of interest. A wide review on this topic is presented by Mignan (2008). In the following, we will
23 describe *M8*, *RTP* (Reverse Tracing of Precursors), *PI* (Pattern Informatics) and *R-AMR* (Revised
24 Accelerating Moment Release). The latter method is the most recent and is the one we know much
25 better, because some of the present co-authors have introduced the corresponding technique (De
26 Santis et al., 2015b). For this reason, we will dedicate a specific section to it.

27

28

29

30 *M8*

31

32 *M8* was called in this way because it was designed by retroactive analysis of the seismicity
33 preceding the greatest (*M8+*) EQs worldwide (e.g. Keilis-Borok and Kossobokov, 1990;
34 Kossobokov, 2013). Some spatio-temporal functions are introduced in order to reconstruct a 7-



1 dimensional phase space (the first three quantities are estimated for two values C of the average
2 annual number of earthquakes in the sequence; usually $C=10$ and 20): $N(t)$ is the number of main-
3 shocks; $L(t)$ the deviation of $N(t)$ from the long-term trend; $Z(t)$ the linear concentration of the main-
4 shocks; and $B(t)$ is the maximal number of aftershocks as a measure of EQ clustering (these
5 functions are actually properly normalized). The algorithm then recognizes a well established
6 criterion, defined by extreme values of the phase space coordinates, as a vicinity of the system
7 singularity. When a trajectory enters the criterion, probability of extreme event increases to the level
8 sufficient for its effective provision, so an alarm or a TIP, “Time of Increased Probability”, is
9 declared. This algorithm can be adapted for lower magnitudes and particular regions (e.g. CN8).

10

11 *The Reverse Tracing of Precursors (RTP)*

12

13 The *RTP* is a method for medium-term (some months in advance) EQ prediction (Shebalin et al.,
14 2006), which is based on a hierarchical ensemble of premonitory seismicity patterns. These patterns
15 are: (1) “precursory chains” that are related with the correlation length (e.g. Zoller and Hainzl, 2002,
16 Tyupkin and Di Giovambattista, 2005), (2) “intermediate-term patterns” that could be related to
17 some accelerating seismicity (e.g. Gabrielov et al., 2000) and (3) “pattern recognition of infrequent
18 events” that take into account several “opinions” to decide the validity of the calculated chain of
19 events. If a sufficient number of “votes” is accumulated, then the chain is considered precursory
20 (Shebalin et al., 2006). Some past EQs seem to have been predicted 6 to 7 months in advance,
21 although a few false alarms also happened. Critical aspects are related to the predicted “area of
22 alarm” that seems very large for a realistic application.

23

24 *Pattern Informatics (PI)*

25

26 The *PI* is a technique for quantifying the spatio-temporal seismicity rate changes in historic
27 seismicity (e.g. Rundle et al., 2002; Nanjo et al. 2005). Tiampo et al. (2006) derive a relationship
28 between the “PI index” and stress change (e.g. Dieterich, 1994), based upon the crack propagation
29 theory. In practice, the PI method measures the change in seismicity rate at each box of a pre-
30 defined grid, relative to the background seismicity rate, through the division of the average rate by
31 the spatial variance over all boxes. Then it identifies the characteristic patterns associated with the
32 shifting of small EQs from one location to another through time prior to the occurrence of large
33 EQs (Tiampo et al., 2006). Results are given in terms of mapping the “PI anomalies” which are



1 located where a new large EQ can be expected. Holliday et al. (2007) have proposed a modification
2 of PI by using complex eigenfactors, explaining the EQ stress field as obeying a wave-like equation.

3

4

5 **4. Shannon Entropy and Shannon Information**

6

7 The Shannon Entropy $h(t)$ (Shannon, 1948) is an important tool for the space-time characterization
8 of a dynamical system. In general, for a system characterized by K possible independent states, this
9 entropy is defined in a certain time t as follows:

$$10 \quad h(t) = -\sum_{i=1}^K p_i(t) \cdot \log p_i(t) \quad (1)$$

11 where $p_i(t)$ is the probability of the system to be at the i -th state. For convenience, we impose

12 $\sum_i p_i = 1$ and $\log p_i = 0$ if $p_i = 0$ to remove the corresponding singularity.

13

14 In literature, we can find a large number of physical interpretations of the Shannon Entropy. We
15 consider here what we think it is the simplest one: it is a non-negative measure of our ignorance
16 about the state of the system of concern. The Shannon Entropy has a great importance in evaluating
17 and interpreting the behaviour of complex systems like Earth, in general, and EQs, in particular. On
18 the other hand, we find in literature also the Shannon Information, $I(t)$, which is simply related to
19 $h(t)$ as $I(t) = -h(t)$. Consequently, the Shannon information is a negative quantity that measures our
20 knowledge on the state of the system when we know only the distribution of probability $p(t)$ (Beck
21 and Schlögl, 1993). Thus, this quantity measures our decreasing ability to predict the future
22 evolution of the system under study.

23

24

25 **5. Gutenberg-Richter law and b -value**

26

27 The Gutenberg-Richter (GR) law has a central role in seismology (Gutenberg and Richter, 1944). It
28 expresses the (decimal logarithm of the) cumulative number n of EQs with magnitude m equal to or
29 larger than a magnitude M :

30

$$31 \quad \log n(m \geq M) = a - bM \quad (2)$$



1 as a simple linear function of the magnitude M ; a and b are two constant parameters for a certain
 2 region and time interval, characterizing the associated seismicity; in particular, b is the negative
 3 slope of the above cumulative distribution and typically $b \approx 1$. Very soon it was recognized the
 4 importance of estimating the b -value as an indicator of the level of stress in a rock from laboratory
 5 experiments (Scholz, 1968), and only later the relationship has been confirmed for EQs
 6 (Schorlemmer et al., 2005).
 7 Aki (1965) was the first to provide a simple expression to estimate b by means of the maximum
 8 likelihood criterion (with a correction proposed by Utsu, 1978):

$$9 \quad b = \frac{\log e}{\bar{M} - M_{\min} + \Delta/2} \quad (3)$$

10 with an uncertainty of $\pm b/\sqrt{N}$; N is the total number of analyzed EQs; $e = 2,71828 \dots$ is the Euler
 11 number, while \bar{M} is the mean value of the magnitudes of all considered EQs; M_{\min} is the minimum
 12 magnitude used in the b -value evaluation; Δ is the resolution involved in the magnitude estimation,
 13 normally $\Delta=0.1$. Usually the M_{\min} is the magnitude of completeness of a seismic catalog, i.e. the
 14 magnitude threshold at which or above the corresponding seismic catalog includes all occurred EQs
 15 in the region.

16

17 **6. Entropy and EQs**

18

19

20 Now we apply the concept of Shannon Entropy to EQs. Most of this section is based on De Santis
 21 et al. (2011a) with some extension in order to clarify some concepts.

22

23 Given a sequence of EQs (in the form of a seismic catalog or a seismic sequence within a certain
 24 region) with non-negative (and normalized) probability P_i to have activated a certain i -th class of
 25 seismicity characterized by some range of magnitudes, the associated non-negative Shannon
 26 entropy h can be defined as (De Santis et al., 2011a):

$$27 \quad h = -\sum_{i=1}^K P_i \cdot \log P_i \geq 0 \quad (4)$$

28 Since eq. (4) is applied to a discrete number of states, h is also called *discrete Shannon entropy*. It
 29 can be considered a reliable measure of uncertainty and missing information of the system under
 30 study.

31



1 Actually, the values of magnitude can assume a continuous range (in theory from M_{min} to infinity)
2 then the discrete definition (4) becomes an integral definition (Shannon, 1948; Ihara, 1993):

$$H = - \int_{M_{min}}^{\infty} p(M) \cdot \log p(M) dM \quad (4a)$$

3
4 where H is now called *continuous* (or *differential*) *Shannon entropy* to be distinguished from h , and
5 $p(M)$ is the probability density function (*pdf*) of the magnitudes M , such as

$$p(M) = \frac{d}{dm} \sum_{i, m \leq M} P_i(m)$$

6
7 and

$$\int_{M_{min}}^{\infty} p(M) dM = 1$$

8
9
10 It is worth noticing that moving from the discrete definition (4) to the continuous (4a), the property
11 of non-negative h is lost by H , that can assume also negative values (e.g., Ihara, 1993). This is not
12 evident from the work by De Santis et al. (2011a), so we will spend here some words about it.

13
14 The two definitions of the Shannon entropy are related by the following equation:

$$H = h + \log \Delta \quad (5)$$

15
16 where Δ is the sampling step of the continuous *pdf* in order to let it discrete in h (e.g. Klir 2006). It
17 is evident from (5) that when Δ tends to zero, H will diverge to $-\infty$. Thus, the continuous entropy H
18 is not a limit for $\Delta \rightarrow 0$ of the Shannon discrete entropy h and, consequently, it is not a measure of
19 uncertainty and information. However, the continuous Shannon entropy can be used to measure
20 differences in information (Ihara 1993).

21
22 However, when the classes of magnitude are loose, e.g. for $\Delta \approx 1$ we will have $H \approx h$: De Santis et al.
23 (2011a) considered $\Delta = 0.5$ so the difference between discrete and continuous entropies was only 0.3.

24
25 De Santis et al. (2011a) have shown that if the $p(M)$ is the GR probability distribution, then H can
26 be expressed in terms of the b -value:

$$H \approx 0.072 - \log b \quad (6)$$

27
28
29
30 This relation is detailed and proved in the Appendix.

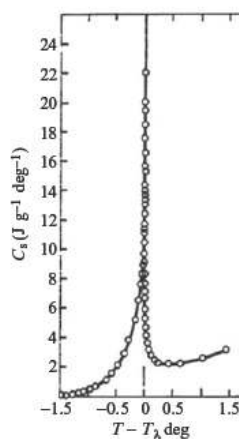


1

2 7. Entropy and critical point theory

3

4 An *ergodic* dissipative system can have a critical point where the system undergoes through a
5 transition. The ergodic property means that the system averages in real 3D space are equivalent to
6 averages in the ideal reconstructed phase space (e.g. Takens, 1981, De Santis et al., 2011b). As an
7 example, Fig. 1 reports the behaviour of the *specific heat* around a critical point occurring at
8 temperature T_λ degree. It is interesting how the system approaches the critical temperature as a
9 power law. In addition, if the system changes its temperature linearly in time, the same plot is
10 expected versus time.

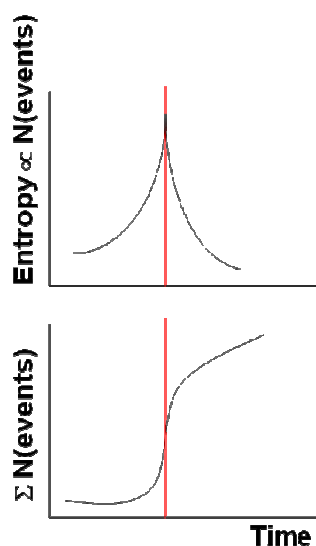


11

12 **Fig. 1.** Specific heat of ^4He as a function of $T - T_\lambda$ in Kelvin. T_λ is the temperature at which the critical system has a
13 transition (critical point) (Adapted from Stanley, 1971).

14

15 More generally, if we replace the increasing temperature with the system entropy, then the system
16 reaches its critical point (vertical red line in Fig.2) at the largest Entropy and approaches it with an
17 accelerating power law in its cumulative of *punctuated* events (we intend here for an “event” as an
18 anomalous behaviour of the system evolution, e.g. when its signal level is larger than a certain
19 number of standard deviation, σ , e.g. 2.5σ).



1

2 **Fig. 2.** Idealized Shannon entropy (above diagram) and cumulative number of events (bottom diagram) for a dissipative
3 system around its critical point, indicated by the vertical red line.

4

5

6 After the critical point, the curve behaves as a decelerating power law. Fig. 2 depicts both the
7 idealized behaviours for the entropy and the cumulative number of events.

8 We will see in the following how these patterns are reproduced in the case studies of some Italian
9 seismic sequences.

10

11 **8. Entropy studies of two Italian seismic sequences**

12

13

14 In this part, we show two case studies in Italy: the 2009 L'Aquila and the 2012 Emilia seismic
15 sequences, both producing a main-shock of around M6 (precisely local and moment magnitudes,
16 ML5.9 and Mw6.2 for L'Aquila and local magnitude ML5.9 for Emilia). Main characteristics of the
17 two seismic sequences are given in Table 1. The first case was already analysed and discussed by
18 De Santis et al. (2011a). However, we will make here some alternative/complementary analyses,
19 with respect to those already published. The second case study is original and never published so far.

20

21

22



Sequence ID	Main-shock Parameters						# data (foreshocks)	R_{\max} (km)	M_{\min}
	Coord. (lat, lon) in degree	Depth (km)	Date	t_f in days from 1 May 2005 (predicted)	Fault style	Magnitude (predicted) *			
L'Aquila	42.34N 13.38E	8.3	6 Apr 2009	1436.06 (1437.4)	N	5.9 (5.3±0.5)	17	300	4.0
Emilia	44.89N 11.23E	6.3	20 May 2012	2576.09 (2577.7)	R	5.9 (5.7±0.5)	38	300	4.0

* normally deduced from eq. (2a or 2b)

1 **Table 1** - Main data related to the two Italian seismic sequences under study: (from left to right) the label, the main-
 2 shock source parameters, the number of data points (foreshocks) used in the fitting stage; the maximum distance from
 3 the main-shock epicentre defining the selection area and the minimum threshold magnitude of the selected events there
 4 considered. We provide also a rough estimation of the predicted magnitude (within brackets) of the impending main-
 5 shock (see text). N and R in the Fault style column stand for Normal, and Reverse focal mechanism, respectively. R_{\max}
 6 and M_{\min} are the largest area and minimum magnitude, respectively, considered in the analyses.

7

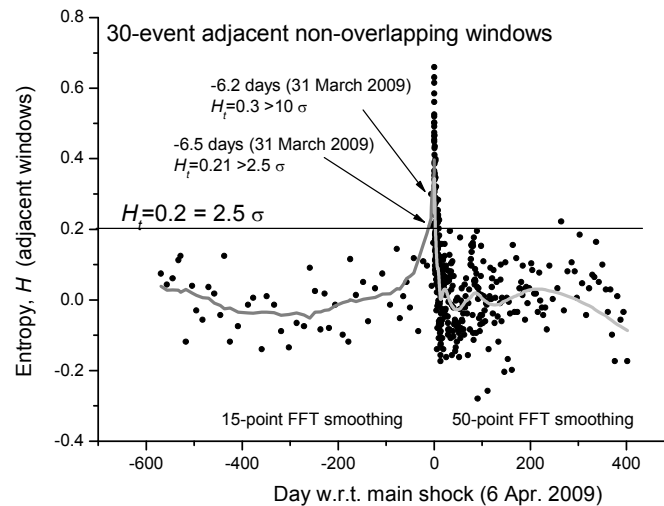
8 *The 2009 L'Aquila seismic sequence*

9

10 As mentioned in De Santis et al. (2011a), Shannon entropy can be estimated in three different ways:
 11 cumulative, moving overlapping or distinctively temporal windows. For the first case study, i.e. the
 12 2009 L'Aquila (Central Italy) seismic sequence, we will consider adjacent non-overlapping moving
 13 windows. In Fig.3 we show the estimation of the Shannon Entropy based on non-overlapping
 14 windows of 30 $M_{1.4+}$ seismic events occurred in a circular area of 80 km around the main-shock
 15 epicentre. The low number of events used for the analysis in each window was chosen to better
 16 follow even shorter fluctuations of entropy, especially for the foreshocks. It is interesting that two
 17 distinct entropy values before the main-shock occurrence are larger than the threshold $H_t = 2.5 \sigma$ (the
 18 mean value of entropy, $\langle H \rangle$, is practically zero). To better visualize the mean behaviour of entropy,
 19 the gray curve defines a reasonable smoothing of the entropy values: 15-point FFT before the main-

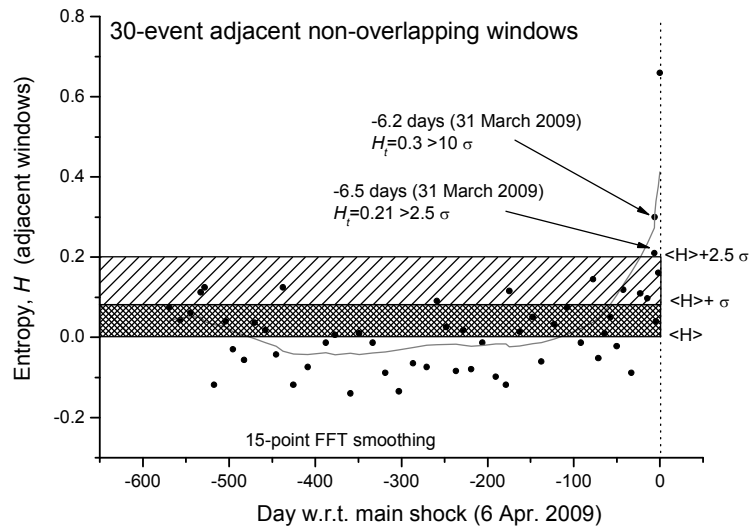


1 shock and 50-point FFT smoothing after the main-shock. The different kind of smoothing is related
2 to the different rate of seismicity before and after the main-shock. It is interesting to notice that the
3 smoothed gray curve of the Shannon Entropy reproduces the expected behavior of a critical system
4 around its critical point (as shown in Fig. 1, but with time as x -axis), with the main-shock as critical
5 point.
6



7
8 **Fig. 3.** Shannon entropy for L'Aquila seismic sequence from around 1.5 year before the main-shock to around 1 year
9 after, calculated for a circular area of 80 km around the main-shock epicenter. Each point is the entropy analysis based
10 on non-overlapping windows, each composed by 30 foreshocks. The gray curve defines a reasonable smoothing of the
11 entropy values: 15-point FFT before the main-shock and 50-point FFT smoothing after the main-shock. The different
12 kind of smoothing is related to the different rate of seismicity before and after the main-shock. It is interesting how the
13 smoothed curve reproduces the expected behavior of a critical system around its critical point. (Adapted from Wu et al.
14 2016).

15
16 We can even analyse in more detail the same curve, but expanded in the period before the main-
17 shock (Fig. 4). We confirm that, around 6 days before the main-shock, there is the persistence of
18 two consecutive values of entropy greater than 2.5σ (the larger value is even greater than 10σ). An
19 interesting question to better investigate in more case studies will be: could this persistence of larger
20 values of entropy be considered a reliable precursor of the imminent main-shock?
21



1
 2 **Fig. 4.** Detail of the Shannon entropy for L'Aquila seismic sequence from around 1.5 year before the main-shock to the
 3 main-shock occurrence. Each point is the entropy analysis based of non-overlapping windows, each composed by 30
 4 foreshocks. The mean value of the entropy, $\langle H \rangle$, which is almost zero, and one and two standard deviations are also
 5 shown. The gray curve defines a reasonable smoothing of the entropy values with 15-point FFT.

6

7 *The 2012 Emilia seismic sequence*

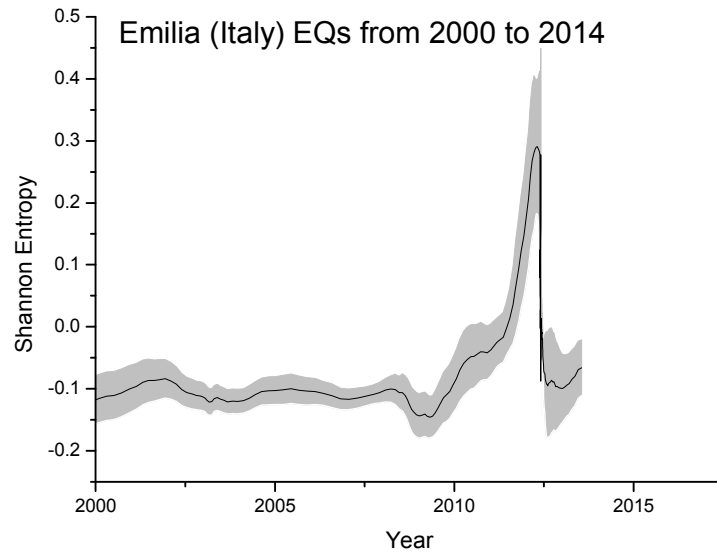
8

9 In this specific case study, we will consider moving and partially overlapping windows, each
 10 composed of around 200 seismic events and overlapping of 20 events. This kind of analysis allows
 11 us to have directly a smoother curve of entropy, without resorting to a subsequent smoothing
 12 operation as done instead in the previous case.

13

14 In Fig. 5 we plot the Shannon entropy for Emilia seismic sequence from 2000 to 2014, as estimated
 15 over all M2+ EQs occurred around 150 km the first major EQ. The significant increase starting
 16 around 2010 is probably real and related to the preparation phase of the two major EQs occurred on
 17 20 and 29 May, 2012 with local magnitudes 5.9 and 5.8, respectively, where the entropy reaches the
 18 maximum value (in this case around 0.3). The gray area defines the estimated error in computing
 19 the entropy.

20



1
 2 **Fig. 5.** Shannon entropy for Emilia seismic sequence from 2000 to 2014. The significant increase from around 2010,
 3 with the maximum at around the main-shock occurrence, is expected to be real. The gray area defines the statistically
 4 estimated (1 standard deviation) error in computing the entropy.

5
 6 **9. Accelerated Moment Release revisited: the case of L'Aquila and Emilia EQs**

7
 8 Benioff (1949) proposed a simple way to estimate the strain-rebound increment, ε_i :

$$s_i = \sqrt{E_i} = k_i \cdot \varepsilon_i \quad (7)$$

10 where E_i is the energy released by the EQ, i.e. $10^{\alpha M + \beta}$ ($\alpha=1.5$, $\beta=4.8$ for energy expressed in Joule,
 11 although Benioff used slightly different values), and $k_i = (\mu P V_i / 2)^{0.5}$ (μ =shear or rigidity modulus,
 12 V_i = volume of the i -th fault rocks, P is the fraction of energy transmitted in terms of seismic waves;
 13 usually it is considered $P \approx 1$). This theory is based on Reid (1910) arguments of the elastic rebound.
 14 To take account of the cumulative effect of a series of N EQs at the time t of the last N -th EQ,
 15 Benioff introduced therefore what is now called *cumulative Benioff strain* s :

$$s(t) = \sum_{i=1}^{N(t)} s_i = \sum_{i=1}^{N(t)} \sqrt{E_i} = 10^{\beta} \sum_{i=1}^{N(t)} 10^{0.75 M_i} \quad (8)$$

17 with $\beta' = \beta/2 = 2.4$. It is important to notice that, according to Benioff (1949), the cumulative strain
 18 (8) is that accumulated *on the fault* under study.



1 Extending the meaning of (8) to the strain accumulated over a larger area around the epicentre, Bufe
 2 and Varnes (1993) obtained interesting results with the so-called *Accelerating Moment Release*
 3 (*AMR*) approach that consists in fitting the cumulative value $s(t)$ expressed as in (8), with a power
 4 law in the time to failure t_f , i.e. the theoretic time of occurrence of the main shock: $s(t)=A+B(t_f - t)^m$,
 5 where A , B and m are appropriate empirical constants (m is expected between 0 and 1: typical value
 6 is 0.3; Mignan, 2008). The fitting process gives as an outcome the time t_f together with the
 7 expected magnitude, which is related to either A or B :

$$8 \quad M_p(A) = \frac{\log(\Delta s_{last}) - \beta'}{0.75} \quad (9a)$$

9 where $\Delta s_{last} = A - s_{last}$ and s_{last} is the cumulative Benioff strain at the last precursory event
 10 considered (namely the N -th EQ). In this expression one speculates that the main-shock will be the
 11 next EQ striking after the N -th, but the occurrence of many smaller EQs after the last analysed
 12 shock and before the predicted time t_f cannot be excluded.

13 An alternative formulation, based on the parameter B , has been given by Brehm & Braile (1999):

$$14 \quad M_p(B) = \frac{\log|B| - \beta' - 0.14}{0.738} \quad (9b)$$

15
 16 A criticism to this method came from Hardebeck et al. (2008) who pointed out the arbitrariness in
 17 the critical choice of the temporal and spatial criteria for data selection, i.e. the initial precursory
 18 event of the *AMR* curve and the extension of the inspected region.

19
 20 To circumvent this criticism, De Santis et al. (2015) introduced what they called R-AMR, i.e. the
 21 Revised Accelerating Moment Release (R-AMR), as a better way of applying the AMR by
 22 weighting the EQs magnitudes in a certain area, according to an appropriate attenuation function
 23 $G=G(R)$, where R is the distance of a given EQ epicentre with respect to the *impending slipping*
 24 *fault*. In particular, the Benioff Strain produced at the fault level is expressed by a reduced Benioff
 25 strain $\hat{s}(t)=s \cdot G$ called “reduced” because the action of the function G , which is normally less than
 26 unity (i.e. $G \leq 1$), is to lower the value of the typical Benioff strain, normally according to the
 27 distance R from the centre of the region of study. As area of interest, a circle is taken with the
 28 corresponding Dobrovolsky radius, $r(\text{km})=10^{0.43M}$ with M =EQ magnitude (Dobrovolsky et al.,
 29 1979).

30

31 Thus, the expression for the cumulative *reduced* strain becomes:

32



$$1 \quad \tilde{s}(t) = \sum_{i=1}^{N(t)} \tilde{s}_i = \sum_{i=1}^{N(t)} \sqrt{E_i} \cdot G(R_i) = 10^{\beta'} \sum_{i=1}^{N(t)} 10^{0.75M_i} G(R_i) \quad (8b)$$

2

3 De Santis et al. (2015b) applied with success their revisited method to the three most important
 4 seismic sequences occurred in Italy in the last ten years. In addition, they also showed that, for a
 5 particular seismic swarm (i.e. with no mainshock), R-AMR performs better than AMR, not
 6 providing a false alarm.

7

8 *R-AMR for the 2009 L'Aquila and 2012 Emilia seismic sequences*

9

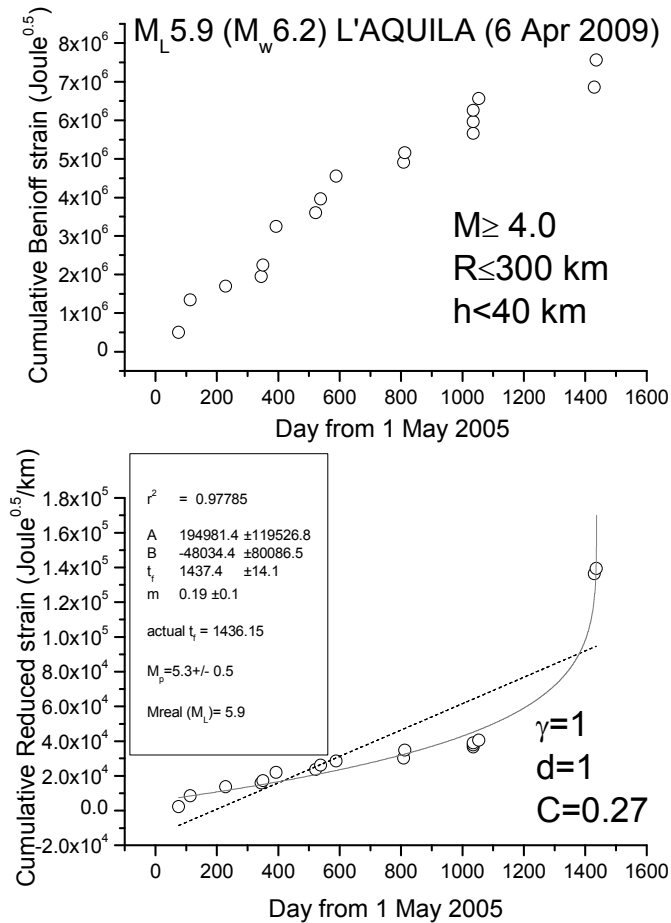
10 We show here two case studies, L'Aquila and Emilia seismic sequences, where the application of
 11 R-AMR is made much simpler than the one firstly proposed in De Santis et al. (2015b). Although
 12 that way of applying of R-AMR is more rigorous because all EQs above the minimum magnitude of
 13 completeness are considered, we show here that a simpler application is possible, where considering
 14 a very simple attenuation function of the form $G(R_i) = d/R_i^\gamma$, with d (normally 1km), R_i in km and
 15 with $\gamma \approx 1$, at the cost of considering a larger minimum magnitude threshold of around M4. Figs 6a
 16 and 6b show the results for the cases of L'Aquila and Emilia sequences, where we apply to all
 17 shallow (depth $h \leq 40$ and $h \leq 80$ km, respectively) M4+ EQs both AMR and R-AMR analyses (top
 18 and bottom of each figure, respectively). Then, we then consider a 300 km size for the regions
 19 where we applied R-AMR analysis. This size is comparable with the corresponding Dobrovolsky's
 20 radius. Both the analyses stop well before the main-shocks that are not so considered in the
 21 calculations. We notice that the time of preparation is rather long for both sequences, i.e. practically
 22 starting at the beginning of the whole period of investigation (May 2005). This fact could be simply
 23 interpreted as the larger foreshocks anticipate the beginning of the seismic acceleration with respect
 24 to the smaller ones, which were the most in the previous analyses in De Santis et al. (2015b).

25 The goodness of the power law fit with respect to the linear regression can be quantified by the C-
 26 factor which is the square root of the ratio between the RMS of the power law and the RMS of the
 27 best linear fit (Bowman et al., 1998): the lower the C-factor than 1, the better the power law fit is
 28 with respect to the line.

29

30

31

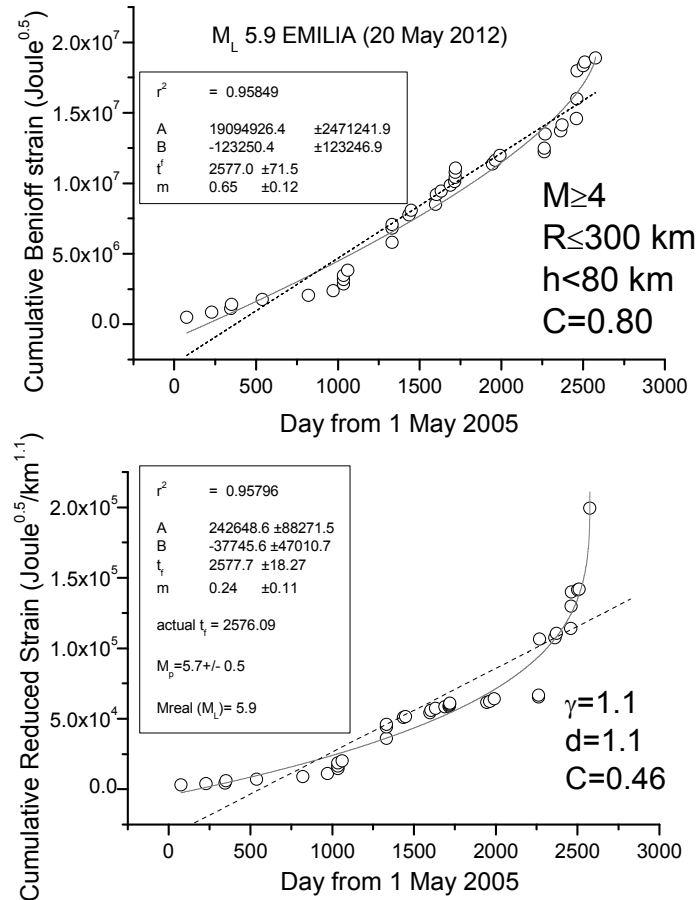


1

2 **Figure 6a** — Analyses of L'Aquila seismic sequence $M \geq 4$ EQs (main-shock not shown and not used in the analysis):
 3 top) ordinary AMR method; bottom) R-AMR method. Dashed line represents the best linear fit, while solid gray curve
 4 is the best power law fit. Results of the fit are shown in the frame inside the graph at the bottom; r^2 is the coefficient of
 5 determination, providing a measure of the quality of the fit (the closer to 1, the better the fit).

6

7 We find a clear seismic acceleration for both seismic sequences, quantified by a low value of C
 8 (0.27 for L'Aquila sequence and 0.46 for Emilia sequence) and a great determination coefficient
 9 ($r^2 > 0.95$ in both cases). In addition, the predicted magnitudes are comparable with (although lower
 10 than) the real ones. In both cases, the beginning of clear acceleration starts around 1.5 year before
 11 the main-shock.



1
 2 **Figure 6b** — Analyses of Emilia seismic sequence $M \geq 4$ EQs (main-shock not shown and not used in the analysis): top)
 3 ordinary AMR method; bottom) R-AMR method. Here the ordinary ASR also showed a little acceleration (C -
 4 factor=0.80) but the R-AMR version is much better (C -factor=0.46). Dashed line represents the best linear fit, while
 5 solid gray curve is the best power law fit. Results of the fit are shown in the frames inside the graphs; r^2 is
 6 the coefficient of determination, providing a measure of the quality of the fit (the closer to 1, the better the fit).

7

8

9 **10. Lithosphere-Atmosphere-Ionosphere Coupling (LAIC)**

10

11 Geosystemics sees the planet in its entirety, where all geo-layers “communicate” each other, in
 12 terms of exchange of matter and/or energy, i.e. what Bekenstein (2003) called with the more generic
 13 term of “information”. An important recent model is the so-called Lithosphere-Atmosphere-



1 Ionosphere Coupling (LAIC) for which before a large EQ, in its preparation phase, some precursory
2 anomalies can appear in atmosphere and/or in ionosphere (e.g. Pulinetts and Boyarchuk, 2004).

3

4 The state of the ionosphere is particularly sensitive to the LAIC. Its presence as ionised layer at 50-
5 1000 km altitude above the Earth's surface is important to detect any electromagnetic change in the
6 circumterrestrial environment (Kelley, 2009). Comprehensive reviews of the papers describing the
7 measurements of the seismo-ionospheric signals are reported in De Santis et al. (2015b) and Jin et
8 al. (2015). In addition, Pulinetts and Davidenko (2014) make a discussion on the temporal and
9 spatial variability of the ionospheric precursor summarizing the results obtained by a large number
10 of authors so far. In particular, they describe in detail which is the role of the Global Electric Circuit
11 in transferring information from the Earth's surface up to the ionosphere.

12

13 The finding of atmospheric anomalies prior to large EQs is more recent and also debated as well.

14

15 In this section, we remind some of those phenomena, the nature and characteristics of which are
16 more directly of interest for the understanding of LAIC.

17

18 *Pre-EQ ionospheric evidences from ground-based observations*

19

20 A coupling (post-seismic) effect of an EQ to the above atmosphere is already well known: it can
21 appear just after the occurrence of a sufficiently large event, and it is related to the possibility of
22 observing the effect of the propagation of acoustic gravity waves in the ionosphere (e.g. Row, 1967).
23 Recently, this effect has been clearly detected as wave-like fluctuations of the Total Electron
24 Content (TEC) in ionosphere 21 minutes after the April 25, 2015 M7.8 Nepal EQ
25 (<http://gpsworld.com/gps-data-show-how-nepal-quake-disturbed-earths-upper-atmosphere/>;
26 last access on 23 October 2017).

27

28 Important precursory effects of LAIC before large EQs can be detected in the ionosphere from
29 ground-based observational systems like ionosondes and GPS (Global Positioning System)/GNSS
30 (Global Navigation Satellite System) receivers.

31

32 A large number of papers report some variations of ionospheric parameters before many large EQs,
33 such as the F2-layer critical frequency (foF2) (Hobara and Parrot, 2005; Liu et al., 2006; Dabas et



1 al., 2007; Perrone et al. 2010; Xu et al. 2015) and the sporadic E layer (Es) (Silina et al. 2001;
2 Ondoh 2003; Ondoh and Hayakawa 2006).

3

4 The study of foF2 alone is a very “inconvenient” ionospheric parameter for the role of EQ precursor,
5 because, besides the geomagnetic activity effects, there would be many other reasons for non-EQ
6 related foF2 variations. Therefore, a multi-parameter analysis is preferable and some works have
7 analysed more ionospheric parameters at the same time, in order to achieve a more robust result.
8 For instance, in the periods of time preceding all crustal EQs in Central Italy with magnitudes $M >$
9 5.0 and the epicenter depth < 50 km, Perrone et al. (2010) have considered the ionospheric sporadic
10 E layer (Es) together with the blanketing frequency of Es layer (fbEs) and foF2, by analysing data
11 from the ionospheric observatory inside the preparation zone. According to these authors, the found
12 deviations of ionospheric parameters from the background level can be related to the magnitude and
13 the epicentre distance of the corresponding EQ.

14

15 There is significant literature related to the analysis of the ionospheric effects before and during an
16 EQ revealed by GPS/GNSS ground-based measurements, in terms of TEC fluctuations and
17 scintillation anomalies that have been claimed to be detected some days before the EQs. Just to
18 mention the more recent works, Mancini et al. (2014) analysed 5 years of GNSS-based ionospheric
19 TEC data to produce maps over an area surrounding the epicentre of the 2009 L’Aquila EQ. An
20 interesting ionospheric anomaly was found in the night of 16 March 2009, anticipating the main
21 shock by 3 weeks and could be connected with it. Contadakis et al. (2014) reported on the analysis
22 of the total electron content (TEC) from eight GPS stations of the EUREF network by using
23 discrete Fourier to investigate the TEC variations over the Mediterranean region before and during
24 the 12 October 2013 Crete, Greece EQ. Over an area of several hundred kilometers from the EQ
25 epicentre, all stations used in this study observed an increase of 2-6 TECU from 10 October to 15
26 October 2013, likely related to the EQ. Akhoondzadeh (2015) applies a complex algorithm, the
27 Firefly Algorithm (FA), as a robust predictor to detect the TEC seismo-ionospheric anomalies
28 around the time of the some powerful EQs (27 February 2010 M8.8 Chile, 11 August 2012 M6.4
29 Varzeghan and 16 April 2013 M7.7 Saravan). Significant anomalies were observed 3 - 8 days
30 before the EQs.

31 A recent paper by Kuo et al. (2015) presents the application of the LAIC model to compute the TEC
32 variations and compare the simulation results with TEC observations for the Tohoku-Oki EQ (Japan,
33 11 March 2011, Mw 9.0). In the simulations, these authors assumed that the stress- associated
34 current starts ~40 minutes before the EQ, and then linearly increases reaching its maximum



1 magnitude at the time of the EQ main-shock. Comparisons with experimental values suggest that a
2 dynamo current density of $\sim 25 \text{ nA m}^{-2}$ is required to produce the observed variation of $\sim 3 \text{ TECU}$.

3

4 However, it must be noted that the relationship between ionospheric anomalies and electromagnetic
5 signals generated by the EQ preparation is still controversial and highly debated, as demonstrated
6 by the high number of papers reporting re-analysis of data and comments aiming to refute evidences
7 of this correlation. For example, Masci et al. (2015) comment the findings of Heki (2011) and Heki
8 and Enomoto (2013). After a re-analysis of the data, used by Heki (2011) to demonstrate the
9 existence of a TEC anomaly 40 minutes before the EQs (2011 Tohoku-Oki and other $M > 8$ EQs),
10 Masci et al. (2015) conclude that this anomaly is due to an artefact introduced by the choice of the
11 definition of the reference line adopted in analysing TEC variations.

12

13

14 *Pre-EQ ionospheric evidences from in-situ measurements*

15 Although many works on the possible pre-EQ effects in the ionosphere were also made with the
16 early advent of satellites, it was with the DEMETER (Detection of Electro-Magnetic Emissions
17 Transmitted from EQ Regions; 2004-2010) and CHAMP (CHALLENGING Minisatellite Payload;
18 2000-2010) missions that most of the striking results were obtained.

19

20 DEMETER was a French micro-satellite operated by CNES and specifically designed to the
21 investigation of the Earth ionosphere disturbances due to seismic and volcanic activities. It operated
22 for more than 6.5 years of scientific mission (2004-2010). The results from the analyses of this
23 satellite dataset have statistically proved definitively the existence of the LAIC: what is still needed
24 is to understand the deterministic details. Using the complete DEMETER data set (Piša et al. 2013),
25 careful statistical studies were performed on the influence of seismic activity on the intensity of low
26 frequency EM waves in the ionosphere. In the satellite lifetime, several thousands of magnitude
27 $M5+$ EQs occurred so constituting the seismic database. In particular the normalized probabilistic
28 intensity obtained from the night-time electric field data is below the “normal” level, shortly (0 – 4
29 hours) before the shallow (depth $< 40 \text{ km}$) $M5+$ EQs at 1 – 2 kHz. Clear perturbations are observed
30 a few hours before the EQs, as another example of “imminent” forecast: they are real, although they
31 are weak and so far only statistically revealed. No similar effects were observed during the diurnal
32 hours and for deeper EQs. It is interesting also to note that the spatial scale R of the affected area is
33 approximately 350 km confirming relatively well the size of the EQ preparation zone estimated
34 using the *Dobrovolsky et al. (1979)* formula. The main statistical decrease is observed at about 1.7



1 kHz, corresponding approximately to the cut-off frequency of the first transverse magnetic (TM) mode of the Earth–ionosphere waveguide during the night-time. An increase of this cut-off frequency effect would therefore necessarily lead to the decrease of the power spectral density of electric field fluctuations observed by DEMETER in the appropriate frequency range, meaning a lower height of the ionosphere above the epicenter of the imminent EQ. As the EM waves propagating in the Earth-ionosphere wave-guide are mainly whistlers, this means that their propagation is disturbed above the epicenters of future EQs, instead of a change of their intensities.

8
9 Ryu et al. (2014a,b) took advantage of the simultaneous measurements of these two satellites: they analysed the electron density and temperature, ion density composition and temperature data from DEMETER ISL (Langmuir Probe), ICE (Electric Field Instrument) and IAP (Plasma Analyzer Instrument), together with CHAMP PLP data (electron density and temperature) and IONEX maps of $vTEC$ (vertical TEC) from IGS (International GNSS Service). Their aim was the investigation of the ionospheric fluctuations related to the EQs occurred in September 2004 near to the south coast of Honshu, Japan (Ryu et al, 2014a) and Wenchuan EQ (M7.9) of 12 May 2008 (Ryu et al, 2014b). The main result was the detection of a gradual enhancement of the EIA (Equatorial Ionospheric Anomaly) intensity starting one month prior to the event, reaching its maximum eight days before, followed by a decreasing behavior, very likely due to an external electric field generated over the epicenter affecting the existing $\mathbf{E} \times \mathbf{B}$ drifts responsible of the EIA.

20 By analysing the magnetic data from Swarm satellites of the European Space Agency, a recent paper (De Santis et al. 2017) finds some important patterns before the April 25, 2015 M7.8 Nepal EQ, that resemble the same obtained from the seismological analysis of the foreshocks.

24 *Pre-EQ atmospheric evidences*

25 The improvement and increase of satellite remote sensing missions go back to early 1980's. Since then, evidences of many types of infrared (IR) physics parameters have been recognized as useful to identify possible pre-EQ anomalies. Among them, the most cited are the Brightness Temperature (BT), Outgoing Longwave Radiation (OLR), Surface Latent Heat Flux (SLHF), Skin Surface Temperature (SST), and the atmospheric temperature at different altitudes. Although the topic is still debated or even controversial, many scientists agree that those parameters could change before EQs and so they are regularly recorded by satellite at regional and global scales. Examples of such variations of temperature or aerosols can be found in Pulinets et al. (2006), Jing et al. (2013), and Akhoondzadeh (2015). BT corresponds to the temperature of a black body that emits the same intensity as measured, and Xie and Ma (2015) found a clear BT anomaly in correspondence of



1 Lushan M7 EQ (China). OLR is the emission of the terrestrial radiation from the top of the Earth's
2 atmosphere to the space; it is controlled by the temperature of the earth and the atmosphere above it,
3 in particular, by the water vapor and the clouds: as examples, Ouzounov et al. (2011) reported
4 anomalies in this parameter days before the seismic events. SLHF describes the heat released by
5 phase changes and shows an evident dependence on meteorological parameters such as surface
6 temperature, relative humidity, wind speed, etcetera. SST is the temperature of the Earth's surface
7 at radiative equilibrium (usually, the interface between soil and atmosphere, on lands; it is identical
8 to Sea Surface Temperature over the seas), in contrast with the meteorological definition of surface
9 temperature measured by air thermometers which take readings at approximately 1 meter above
10 ground level. We will study the SST for the epicentral areas of the L'Aquila and Emilia main-
11 shocks.

12

13 The nature of the detected IR anomaly as a real temperature change, or perhaps just an emission in
14 the IR frequency band, is a debated issue. In a recent paper, Piroddi et al. (2014) show a clear
15 Thermal IR (TIR) anomaly preceding the 2009 M6.2 L'Aquila (Italy) EQ. The authors propose a
16 mechanism of generation of electric currents in the lithospheric rocks when they are under stress
17 and a consequent IR irradiation with no actual temperature change (e.g. Freund, 2011). However,
18 some recent works identified SLHF (Qin et al., 2011) and surface temperature anomalies (Qin et al.,
19 2012) occurring before large EQs, thus supporting the possibility for some actual change of
20 temperature too. Although the exact cause of such temperature raise is still unknown, it is possible
21 to definitely exclude the radon as a possible direct heat source, on the basis of the results of
22 laboratory experiments conducted by Martinelli et al. (2015). Pulinets et al. (2015) resort to another
23 role of radon as possible indirect source: it could drive particle ionization and aerosol aggregation,
24 where the latent heat release can cause the found increase in the atmospheric temperature.

25

26 Application of particular sophisticated techniques is mandatory to identify the anomalous signal in
27 the TIR data. For instance, Tramutoli (2007, 2010), Aliano et al. (2008), and more recently Xiong et
28 al. (2015) propose some robust satellite techniques that take into proper account the past behaviour
29 of the signal under investigation: the typical seasonal and yearly background is computed and
30 statistically significant deviation from it may represent the thermal anomaly. Recent interest was
31 also addressed to air-quality data as possible indicators of an impending EQ (e.g. Hsu et al., 2010):
32 these authors found a staggering increase in ambient SO₂ concentrations by more than one order of
33 magnitude across Taiwan several hours prior to two (M6.8 and M7.2) significant EQs in the island.

34



1 An interesting, although still controversial, emerging study concerns the EQ clouds (Guangmeng
 2 and Jie, 2013), suggesting that their formation is due to some local weather conditions caused by
 3 energy and particle exchanges between crust and atmosphere able to locally modify the global
 4 electric circuit during the EQ preparation phase (e.g. Harrison et al., 2014); or to create the
 5 conditions for electrical discharges in an atmosphere that may be the source of very high frequency
 6 (VHF) radio-emissions, sometime detected prior to large EQs (Ruzhin and Nomicos, 2007).
 7 Recently, the claim of unusual cloud formation prior strong EQs by Guangmeng and Jie (2013) was
 8 strongly questioned by Thomas et al. (2015) with a counter-analysis based on examination of 4
 9 years of satellite images and correlation analyses between linear-cloud formations and EQ
 10 occurrence.

11

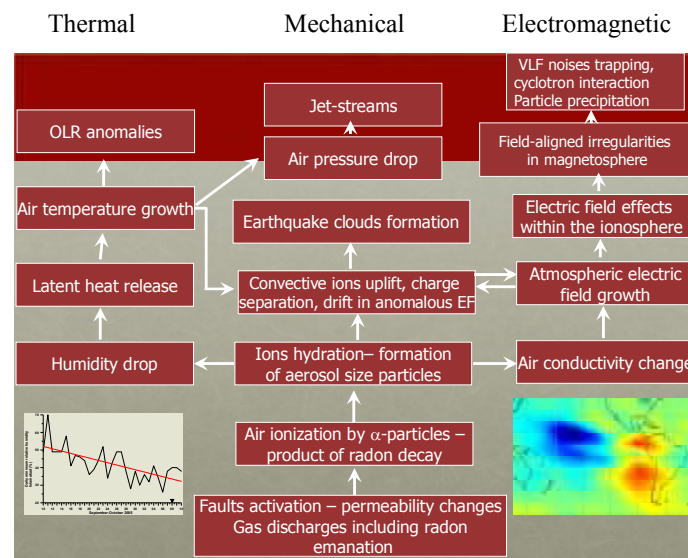
12 *Physical Models*

13

14 A plausible physical omni-comprehensive model justifying the great variety of evidences given
 15 before is the real difficult conundrum for the scientists in this field. There are many theories that
 16 attempt to describe the physical processes manifesting anomalous behaviour in some parameters
 17 before the occurrence of an EQ and try to explain what could cause these precursors. A review of
 18 these processes can be found in Pulinets and Boyarchuk (2004), Freund (2011), Pulinets and
 19 Ouzonov (2011) and the references therein (Figure 7).

20

21



22

23 **Fig.7.** Pulinets-Ouzonov LAIC model (adapted from Pulinets & Ouzonov, 2011; Pulinets et al., 2015)



1
2 Among the many proposed mechanism of generations we can generally classify them as mechanical
3 (atmospheric waves generated by earth motions) and electrical (electric fields in Earth's crust)
4 sources: among the former, we can count the various kinds of atmospheric waves as internal or
5 acoustic gravity waves (IGW and AGW, respectively), planetary waves and tides. In particular, the
6 hypothesis of acoustic gravity waves generation before EQs was proposed by many authors (e.g.
7 Pulinets and Boyarchuk, 2004).
8
9 More complex and intriguing are the mechanisms that describe the anomalous electric field
10 generation. A theory that can explain many observations is based on the emission of a radioactive
11 gas or metallic ions before an EQ, which may change the distribution of electric potential above the
12 surface of the Earth and then up to the ionosphere (e.g., Sorokin et al., 2001).
13
14 Whatever its source is, penetration of the electric field into the ionosphere could induce anomalies
15 in the ionospheric plasma density and/or conductivity, which are observed above seismic zones (see
16 e.g., Liu et al., 2006; Kon et al., 2011). In contrast with this view, Harrison et al. (2010) proposed
17 that radon emitted before an EQ would increase the conductivity of air at ground level and that the
18 ensuing increase of current in the fair weather global circuit would lower the ionosphere. This
19 mechanism is also supported by Pulinets et al. (2015). However, Freund et al. (2009) have
20 estimated that even if radon is coming out the ground in seismic areas, its contribution to the air
21 conductivity is of minor importance relative to the air ionization rate, which can be expected from
22 charge carriers from the rocks, the so-called positive-holes (or p-holes) (Figure 8).
23

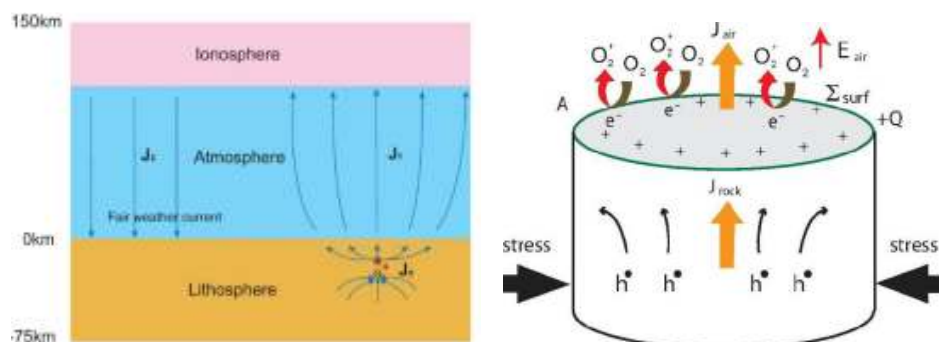
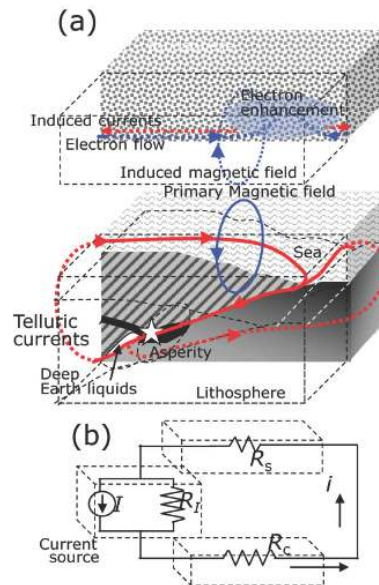


Fig. 8. Freund model (adapted from Kuo et al., 2014)

24
25
26
27



1 They have shown experimentally that these mobile electric charge carriers flow out of the stressed
2 rocks (see Freund et al., 2009, and references therein) and, at the Earth's surface, they cause extra
3 ionization of the air molecules. However, the original experiments that detected these p-holes have
4 been recently contrasted (Dahlgren et al., 2014; but see also Scoville et al., 2015).



5
6

Fig. 9. Enomoto model (adapted from Enomoto, 2012)

7 Kuo et al. (2011, 2014) have shown that ionospheric density variations can be induced by changes
8 of the current in the global electric circuit between the bottom of the ionosphere and the Earth's
9 surface where electric charges associated with stressed rocks can appear. The interaction of the
10 anomalous electric current with the geomagnetic field can even amplify the effect in the higher
11 atmosphere (Kuo et al., 2014).

12 Enomoto (2012; Figure 9) has introduced a fault model that takes account of the couple interaction
13 between EQ nucleation and deep Earth gases, and proposes a physical model of magnetic induction
14 coupling with ionosphere before large offshore EQs.

15

16 11. Examples of thermal coupling before L'Aquila and Emilia EQs

17

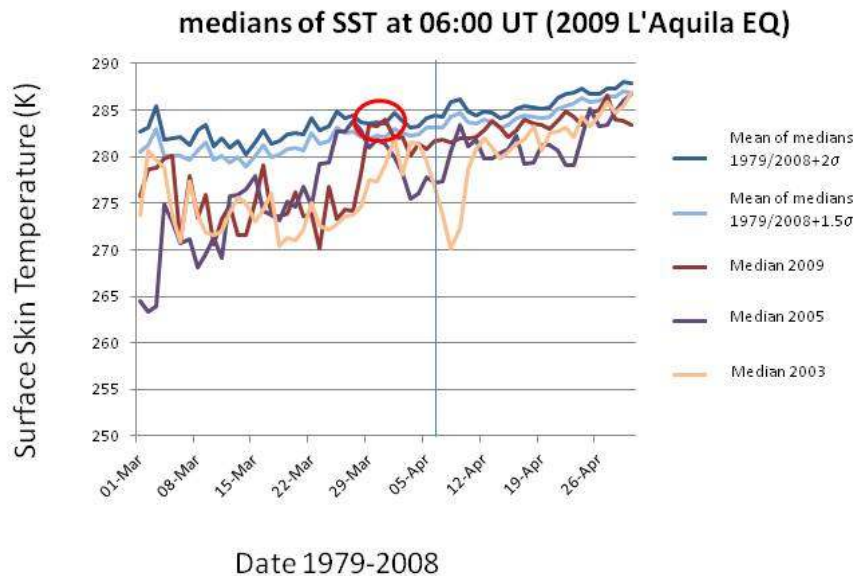
18 In the LAIC model, an important feature should be the coupling between lithosphere and low
19 atmosphere (i.e. the troposphere) in terms of a thermal coupling. As said in the previous section, no
20 general consensus exists about the fact that the thermal anomaly is just an infrared effect (e.g.
21 Freund, 2011) or a real change of temperature (e.g. Qin et al., 2012). We do not want to express



1 here a clear position in this debate. Rather, as didactical examples, we will show some SST studies
2 for the same cases we analysed for the entropy, i.e. the 2009 L'Aquila and the 2012 Emilia
3 sequences of EQs.

4

5 In each case study, we will consider the SST in the epicentral region about two months around the
6 EQ occurrence, and then we will compare the temperatures with those measured in the same day, at
7 the same time (06:00UT) in the time interval 1979-2008 (2011) for L'Aquila (Emilia) EQ. An
8 anomaly of the physical quantity of concern is defined as a value that exceeds the mean (or median)
9 by two times the standard deviation, and persists for at least two days (see also Piscini et al., 2017).



10

11 **Fig. 10.** Median behaviour of 2009 from 1 March to 30 April, compared with all 1979-2008 medians, and particular
12 comparison with 2003 and 2005 medians. All values have been estimated at the epicentre. The red oval indicates when
13 the thermal anomaly in 2009 is larger than or equal to 2 standard deviation, σ (as computed from the previous 1979-
14 2008 years) and persists for at least two days. The vertical line is the EQ occurrence.

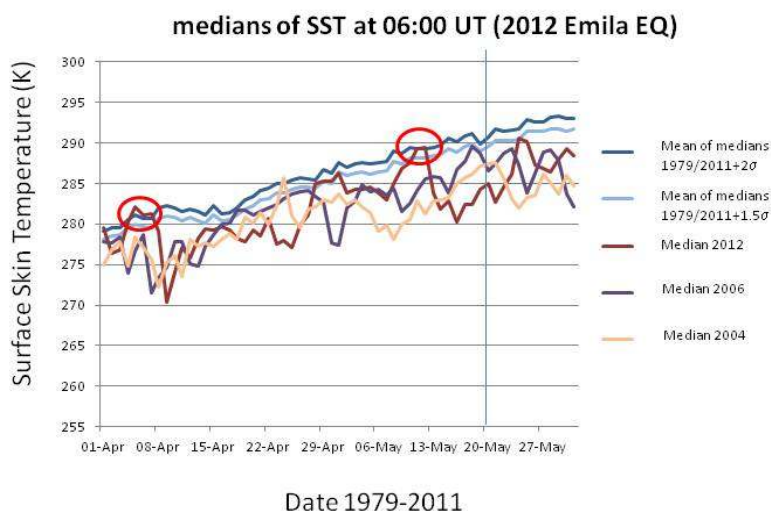
15

16 Fig. 10 and Fig. 11 show the results for the two analyses. In detail, Fig.10 (Fig.11) shows for
17 L'Aquila (Emilia) EQ the median behaviour of 2009, from 1 March (April) to 30 April (31 May),
18 compared with all 1979-2008 (2011) medians, and particular comparison with 2003 (2004) and
19 2005 (2006) medians. For each day the use of the median was preferred because it was thought to
20 be a more robust indicator. The latter years have been used for comparison because no significant
21 seismicity occurred in those years in the two considered regions. All values have been estimated at
22 the EQ epicentre. The red oval indicates when the thermal anomaly in 2009 (2012) is larger than or



1 equal to 2 standard deviations, σ (as computed for each day from the previous 1979-2008 (2011)
2 years) and persists for at least two days. In both analyses, a clear anomaly is found around a week
3 before the EQ occurrence (vertical line in both figures). In the case of Emilia EQ, another persisting
4 anomaly is also found around 1 month and half before the main-shock.

5



6

7 **Fig. 11.** Median behaviour of 2009 from 1 April to 31 May, compared with all 1979-2011 medians, and particular
8 comparison with 2003 and 2005 medians. All values have been estimated at the epicentre. The red ovals indicate when
9 the thermal anomaly in 2012 is larger than or equal to 2 standard deviation, σ (as computed from the previous 1979-
10 2012 years) and persists for at least two days. The vertical line is the EQ occurrence.

11

12 These results confirm some previous studies on the possible thermal coupling in the two EQ cases
13 (e.g. Piroddi et al., 2014; Qin et al., 2012). The same Central Italy showed an analogous thermal
14 anomaly around 40 days before the recent 24 August 2016 M6 Amatrice EQ: Piscini et al. (2017)
15 applied the CAPRI algorithm (CAPRI stands for “Climatological Analysis for seismic PRecursor
16 Identification”) that removes the long-term trend over the whole day by day dataset. This procedure
17 is used mainly to remove a possible "global warming" effect, avoiding to classify as abnormal a
18 more recent year just because of global warming. These authors integrated the analysis of the skin
19 temperature also with total column water vapour and total column of ozone and made a confusion
20 matrix analysis for the last twenty years.

21

22

23



1 12. Mutual Information and Transfer Information: a possible future direction

2

3 Geosystemics focuses on the inter-relations among the components composing the terrestrial
4 complex system. For this reason, every statistical (or physical) quantity that measures these inter-
5 relations is useful. However, given that the system under study is not usually linear, instead of
6 linear quantities such as correlation coefficient or cross-correlation function between two variables
7 belonging to linear processes, we have to resort to statistical quantities, which are more appropriate
8 for nonlinear processes, as typical in a complex system.

9

10 Given two variables X and Y , characterising two processes of the phenomenon under study, we
11 define the mutual information $I(X, Y)$ extending definition (1) to two variables, i.e.:

$$12 \quad I(X; Y) = \sum_{y \in Y} \sum_{x \in X} p(x, y) \cdot \log \left(\frac{p(x, y)}{p_1(x) p_2(y)} \right) \quad (10)$$

13

14 where $p_1(x)$ and $p_2(y)$ are the corresponding probabilities and $p(x, y)$ is the joint probability.

15 However, this formulation does not provide hints about the direction of information transfer
16 between process X and process Y , i.e. from a part of a system to another. For this purpose, it is
17 possible to introduce a useful definition that quantifies the information flow in terms of the
18 Kullback and Leibler entropy (Kullback and Leibler, 1951), which can be defined for a single
19 process X as:

$$20 \quad K_x = \sum_x p(x) \cdot \log[p(x)/q(x)] \quad (11)$$

21 The above quantity is the entropy related to the process X when a different probability $q(x)$ is used
22 instead of the true $p(x)$, and then adapt it in order to be applied to two variables taking into account
23 of a proper delay in one (Schreiber 2000). The so-called transfer information (changing its sign it
24 becomes the transfer entropy) provides also the direction of the information flow.

25 Here, we do not describe more details but we just want to emphasise the importance of quantifying
26 direction of information flow amongst different parts or processes of the system under study,
27 because often it is more important to know where the flow of information is going, instead of just
28 estimating the information that is exchanged by the whole process between internal components or
29 external ones (Ahlsvede et al. 2006).

30

31 Applying this concept to two different time series can be useful to say if one is the master quantity
32 (that represents the causal process) and the other the affected one. In all cases, where we would like



1 to compare/correlate a seismic sequence with possible atmospheric or ionospheric series of
2 precursors, the calculation of the transfer information would provide a robust answer.

3

4

5

6 **13. Conclusions**

7

8 This paper has introduced the concepts of geosystemics, and then has shown its applications to
9 some case studies. The spirit of geosystemics is to use some universal tools to look at some
10 macroscopic quantities, such as the entropy, the Benioff strain, or the temperature to consequently
11 deduce macroscopic properties of the physical system under study. An important frame is that of
12 dynamical systems approaching a critical point, when the macroscopic properties of the system
13 change dramatically. This could be the case of a sequence of EQs that culminates with a main-
14 shock. Therefore, we showed some results obtained with the study of two recent Italian seismic
15 sequences, the 2009 L'Aquila and the 2012 Emilia sequences.

16

17 It is obvious that, being the study of EQs a very complex problem, the more characterizing
18 parameters are analysed, the more robust the result will be. A recent and extensive example of this
19 approach is given by Wu et al. (2016) for the case of the 2009 L'Aquila seismic sequence.

20

21 A further question is how we can use the Big Data in geosciences and, in particular, to analyze
22 precursory patterns of big earthquakes. Of course, the analysis of a greater number of data and the
23 check of multiple models is perceptible that allows to find some type of pattern before an
24 earthquake, that could be likely valid only for regions very localized. An extensive statistical big
25 data analysis would be important to confirm or confute the individual case results. An example of
26 this approach is given by Piscini et al. (2017) where the validity of local climatological variations as
27 possible seismic precursors in Central Italy has been statistically established.

28

29

30

31

32

33

34



1 **Acknowledgements**

2

3 The authors thank ESA (European Space Agency) for funding the SAFE (Swarm for Earthquake
4 study) project under STSE Swarm+Innovation Programme, and INGV (Istituto Nazionale di
5 Geofisica e Vulcanologia) for funding LAIC-U (Lithosphere-Atmosphere-Ionosphere Coupling
6 Understanding) and ECHO (Entropy and CHaOs: tools for studying and characterizing seismic
7 sequences evolution) Projects, under which much work was undertaken for preparing this work.



1 **Appendix: Derivation of Eq. (6)**

2

3 The derivation of eq. (6) is as follows:

4

5 The probability density function corresponding to the Gutenberg-Richter law is

$$6 \quad p(M) = \frac{b \cdot 10^{-b(M-M_{\min})}}{\log e} \quad \text{with } M \geq M_{\min} \quad (\text{A1})$$

7

8 and, imposing $M_{\min} = M_c$, hence:

$$9 \quad H = - \int_{M_c}^{\infty} p(M) \cdot \log p(M) dM = - \int_{M_c}^{\infty} \frac{b \cdot 10^{-b(M-M_c)}}{\log e} \log \left(\frac{b \cdot 10^{-b(M-M_c)}}{\log e} \right) dM =$$

$$10 \quad = - \frac{b}{\log e} \int_{M_c}^{\infty} 10^{-b(M-M_c)} [\log b - b(M - M_c) - \log(\log e)] dM$$

$$11 \quad = - \frac{b}{\log e} \left\{ [\log b - \log(\log e)] \int_{M_c}^{\infty} 10^{-b(M-M_c)} dM - b \int_{M_c}^{\infty} (M - M_c) 10^{-b(M-M_c)} dM \right\}$$

$$12 \quad = - \frac{b}{\log e} \left\{ [\log b - \log(\log e)] \frac{\log e}{b} - b \frac{(\log e)^2}{b^2} \right\} = - \log b + \log(\log e) + \log e,$$

A(2)

13

14 which agrees with equation (6).

15

16



1 **References**

2

3 Ahlswede R., Baumer L., Cao N., Aydinian H., Blinovskiy V., Deppe C., Mashurian H. (Eds.),
4 *General Theory of Information transfer and Combinatorics*, Springer-Verlag Berlin Heidelberg,
5 2006.

6

7 Akhoondzadeh, M. , Ant Colony Optimization Detects Anomalous Aerosol Variations Associated
8 with the Chile Earthquake of 27 February 2010. *Advances in Space Research* 55 (7). COSPAR:
9 1754–63. doi:10.1016/j.asr.2015.01.016, 2015.

10

11 Aki, K. , Maximum likelihood estimate of b in the formula $\log(N) = a - bM$ and its confidence limits,
12 *Bull. Earthq. Res. Inst. Tokyo Univ.*, 43, 237–239, 1965.

13

14 Aki K. and Richards P, *Quantitative Seismology*, 2nd ed., Univ. Science Books, pp. 700, 2002.

15

16 Aliano, C., Corrado, R., Filizzola, C., Genzano, N., Pergola, N., and Tramutoli, V., Robust TIR
17 Satellite Techniques for Monitoring Earthquake Active Regions: Limits, Main Achievements and
18 Perspectives. *Annals of Geophysics* 51 (1): 303–17, 2008.

19

20 Baskoutas, I., Papadopoulos, G.A., Precursory Seismicity Pattern before Strong Earthquakes in
21 Greece. *Research in Geophysics* 4 (1): 7–11. doi:10.4081/rg.2014.4899, 2014.

22

23 Beck, C., and Schlögl, F., *Thermodynamics of Chaotic Systems* (Cambridge University Press,
24 Cambridge 1993) p. 306, 1993.

25

26 Bekenstein, J. D., Information in the Holographic Universe, *Scientific American*, 289, 2, August
27 2003, p. 61, 2003.

28

29 Benioff, H., Seismic evidence for the fault origin of oceanic deeps, *Geol. Soc. Am. Bull.*, 60, 1837-
30 1856, 1949.

31

32 Bizzarri A., On the deterministic description of earthquakes, *Review of Geophysics*, 49, 1-32, 2011.

33



- 1 Bizzarri A., Rupture speed and slip velocity: what can we learn from simulated earthquakes?, *Earth*
2 *Planet. Sci. Lett.*, 317-318, 196-203, 2012.
- 3
- 4 Bizzarri A., The mechanics of seismic faulting: Recent advances and open issues, *La Rivista del*
5 *Nuovo Cimento*, 4, 37, 181-271, 2014.
- 6
- 7 Bowman, D.D., Ouillon, G., Sammis, C.G., Sornette, A., Sornette, D., An observational test of the
8 critical earthquake concept. *J. Geophys. Res.* 103, 24,359–24,372, 1998.
- 9
- 10 Bunde, A., Kropp, J., and Schellnhuber, H. J., *The Science of Disasters*. Climate disruptions, heart
11 attacks, and market crashes, Springer Berlin, 2002.
- 12
- 13 Bufe, C.G., Varnes, D.J. , Predictive modelling of the seismic cycle of the greater San Francisco
14 Bay region, *J. Geoph. Res.*, 98, B6, 9871-9883, 1993.
- 15
- 16 Butz, S. D., *Science of Earth Systems*. Thomson Learning, 2004.
- 17
- 18 Chuvieco E. and Huete A., *Fundamentals of satellite remote sensing*, CRC Press, pp. 448, 2009.
- 19
- 20 Cicerone, R.D., Ebel, J.E., Britton, J. , A Systematic Compilation of Earthquake Precursors.
21 *Tectonophysics* 476 (3-4). Elsevier B.V.: 371–96. doi:10.1016/j.tecto.2009.06.008, 2009.
- 22
- 23 Contadakis, M., Arabelos, D., Vergos, G., Spatalas, S., TEC Variations over Mediteranean before
24 and during the Strong Earthquake ($M = 6.2$) of 12th October 2013 in Crete, Greece. *Phys. & Chem.*
25 *Earth*, 16 (April 2009). Elsevier Ltd: 2319. doi:10.1016/j.pce.2015.03.010, 2014.
- 26
- 27 Dabas, R.S., Das, R.M., Sharma, K., Pillai, K.G.M., Ionospheric precursors observed over low
28 latitudes during some of the recent major earthquakes, *J. Atmos. Solar-Terr. Phys.*, 69, 1813- 1824,
29 2007.



1

2 Dahlgren, P.R., Johnston, M.J.S., Vanderbilt, V.C. and Nakaba, R.N., Comparison of the stress-
3 stimulated current of dry and fluid saturated gabbro samples. *Bull. Seismol. Soc. Am.* 104, 2662–
4 2672, 2014.

5

6 De Santis A., Geosystemics, *Proceedings 3rd IASME/WSEAS International Conference on Geology
7 and Seismology (GES'09)*, Cambridge, 36-40, 2009.

8

9 De Santis A., Geosystemics, entropy and criticality of earthquakes: a vision of our planet and a key
10 of access, in *Nonlinear phenomena in Complex Systems: from Nano to Macro Scale*, ed. E. Stanley
11 and D. Matrasulov, NATO Science for Peace and Security Series – C: Environmental Security, 3-20,
12 2014.

13

14 De Santis A., Qamili E., Geosystemics: a systemic view of the Earth's magnetic field and
15 possibilities for an imminent geomagnetic transition, *Pageoph*, 172, 75-89, 2015.

16

17 De Santis A., Cianchini G., Favali P., Beranzoli L., Boschi E., The Gutenberg–Richter Law and
18 Entropy of Earthquakes: Two Case Studies in Central Italy, *Bull. Seismol. Soc. Am.*, Vol. 101, No. 3,
19 1386–1395, 2011a.

20

21 De Santis A., Qamili E. and Cianchini G., Ergodicity of the recent geomagnetic field, *Physics of
22 the Earth and Planetary Interiors*, 186, 103–110, 2011b.

23

24 De Santis, A., Cianchini, G., Di Giovambattista, R., Accelerating moment release revisited:
25 Examples of application to Italian seismic sequences, *Tectonophysics*, Volume 639, 12 January
26 2015, pag. 82-98, 2015a.

27

28 De Santis et al., Geospace perturbations induced by the Earth: the state of the art and future trends,
29 *Phys. & Chem. Earth*, 85-86, 17-33, 2015b.

30

31 De Santis A. et al., Potential earthquake precursory pattern from space: the 2015 Nepal event as
32 seen by magnetic Swarm satellites, *Earth and Planetary Science Letters*, 461, 119-126, 2017.

33



- 1 Grandy, W.T., Jr, *Entropy and the Time Evolution of Macroscopic Systems*, Oxford University
2 Press, Oxford, 2008.
3
- 4 Gutenberg, B., and C. F. Richter, Frequency of earthquakes in California, *Bull. Seismol. Soc. Am.*,
5 34, 185–188, 1944.
6
- 7 Dieterich, J.H., A constitutive law for rate of earthquake production and its application to
8 earthquake clustering, *J. Geophys. Res.* 99, 2601-2618, 1994.
9
- 10 Dobrovolski, I.P., Zubkov, S.I. & Miachin, V.I., Estimation of the size of Earthquake preparation
11 zones, *Pure appl. Geophys.*, vol. 117, 1025- 1044, 1979.
12
- 13 Dobrovolski, I.P., N.I. Gershenzon, M.B. Gokhberg, Theory of electrokinetic effects occurring at
14 the final stage in the preparation of a tectonic earthquake, *Phys. Earth Planet. Inter.*, 57, 1-2, 144-
15 156, 1989.
16
- 17 Enomoto, Y. , Coupled interaction of earthquake nucleation with deep Earth gases: a possible
18 mechanism for seismo-electromagnetic phenomena. *Geophys. J. Inter.* 191, 1210–1214, 2012.
19
- 20 Favali P., Beranzoli L. and De Santis A. , *Seafloor Observatories: A new vision of the Earth from*
21 *the Abyss*, Springer - Praxis Publishing, 1-2, 2015.
22
- 23 Freund, F.T., Pre-earthquake signals: underlying physical processes. *J. Asian Earth Sci.* 41, 383–
24 400, 2011.
25
- 26 Freund, F.T., Kulahci, I.G., Cyr, G., Ling, J., Winnick, M., Tregloan-Reed, J., Freund, M.M. , Air
27 ionization at rock surfaces and pre-earthquake signals. *J. Atmos. Sol. Terr. Phys.* 71 (17–18), 1824–
28 1834. <http://dx.doi.org/10.1016/j.jastp.2009.07.013>, 2009.
29
- 30 Gabrielov et al., Critical transitions in colliding cascades, *Phys. Rev. E*, 62, N.1, 237-249, 2000.
31



- 1 Guangmeng, G., Jie, Y. , Three attempts of earthquake prediction with satellite cloud images. *Nat.*
2 *Hazards Earth Syst. Sci.* 13, 91–95, 2013.
- 3
- 4 Hardebeck, J.L., Felzer, K.R., Michael, A.J., Improved test results reveal that the accelerating
5 moment release hypothesis is statistically insignificant, *J. Geophys. Res.*, 113, B08310, 2008.
- 6
- 7 Harrison, R.G., Aplin, K.L., Rycroft, M.J., Atmospheric electricity coupling between earthquake
8 regions and the ionosphere. *J. Atmos. Sol. Terr. Phys.* 72, 376–381, 2010.
- 9
- 10 Harrison, R.G., Aplin, K.L., Rycroft, M.J., Earthquake-cloud coupling through the global
11 atmospheric electric circuit. *Nat. Hazards Earth Syst. Sci.* 14, 773– 777, 2014.
- 12
- 13 Heki, K., Ionospheric Electron Enhancement Preceding the 2011 Tohoku-Oki Earthquake.
14 *Geophysical Research Letters* 38 (17): 1–5. doi:10.1029/2011GL047908, 2011.
- 15
- 16 Heki, K., Enomoto, Y. Preseismic Ionospheric Electron Enhancements Revisited. *Journal of*
17 *Geophysical Research: Space Physics* 118 (10): 6618–26. doi:10.1002/jgra.50578, 2013.
- 18
- 19 Hobara, Y., Parrot, M., Ionospheric perturbations linked to a very powerful seismic event, *J. Atmos.*
20 *Solar-Terr. Phys.*, 67, 677–685, doi:10.1016/j.jastp.2005.02.006, 2005.
- 21
- 22 Holliday, J.R., Chen, C.-C., Tiampo, K.F., Rundle, J.B., Turcotte, D.L., Donnellan, A., A RELM
23 earthquake forecast based on pattern informatics. *Seismol. Res. Lett.*, 78, 87–93, 2007.
- 24
- 25 Hough, S., *Predicting the Unpredictable: The Tumultuous Science of Earthquake Prediction.*
26 Princeton University Press, 2009.
- 27
- 28 Hsu, S.C., Huang, Y.T., Tu, J.Y., Huang, Jr-Chung, Engling, G., Lin, C.Y., Lin, F.J., Huang, C.H.,
29 Evaluating real-time air-quality data as earthquake indicator. *Sci. Total Environ.* 408, 2299-2304,
30 2010.
- 31
- 32 Ihara, S. , *Information Theory for Continuous Systems*, World Scientific, London, 1993.
- 33



- 1 Jacobson, M. , R. J. Charlson, H. Rodhe and G. H. Orians (Eds.) *Earth System Science, From*
2 *Biogeochemical Cycles to Global Changes* (2nd ed.). London: Elsevier Academic Press, 2000.
3
- 4 Jing, F., Shen, X.H., Kang, C.L., Xiong, P., Variations of multi-parameter observations in
5 atmosphere related to earthquake. *Nat. Hazards Earth Syst. Sci.* 13, 27-33, 2013.
6
- 7 Kanamori H., The nature of seismicity patterns before large earthquakes, in *Earthquake Prediction*
8 (Simpson D.W and Richards P.G. ed.s), American Geophysical Union, Washington, D.C., doi:
9 10.1029/ME004p001, 1981.
10
- 11 Keilis-Borok, V.I., Kossobokov, V.G., Premonitory activation of earthquake flow: Algorithm M8,
12 *Phys. Earth. Planet. Inter.*, 61, 73-83, 1990.
13
- 14 Kelley M.C., *The earth's ionosphere. Plasma physics and electrodynamics.* 2nd Edition, Elsevier,
15 Amsterdam, 2009.
16
- 17 Klir G.J, *Uncertainty and Information. Foundations of Generalized Information Theory.* J Wiley &
18 Sons, Inc, Hoboken, New Jersey, pp.499, 2006.
19
- 20 Kon, S., Nishihashi, M., Hattori, K., Ionospheric anomalies possibly associated with M_{6.0}
21 earthquakes in the Japan area during 1998–2010: case studies and statistical study. *J. Asian Earth*
22 *Sci.* 41, 410–420, 2011.
23
- 24 Kossobokov, V.G. , Earthquake prediction: 20 years of global experiment, *Nat. Hazards*, 69, 1155-
25 1177, 2013.
26
- 27 Kullback, S., Leibler, R.A., On information and sufficiency. *The Annals of Mathematical Statistics*
28 22 (1), 79–86,1951.
29
- 30 Kuo, C.L., Huba, J.D., Joyce, G., Lee, L., Ionosphere plasma bubbles and density variations
31 induced by pre-earthquake rock currents and associated surface charges. *J. Geophys. Res.* 116,
32 A10317. <http://dx.doi.org/10.1029/2011JA016628>, 2011.
33



- 1 Kuo, C.L., Lee, L., Huba, J.D., An improved coupling model for the lithosphere– atmosphere–
2 ionosphere system. *J. Geophys. Res.* <http://dx.doi.org/10.1002/2013JA019392>, 2014.
3
- 4 Kuo, C. L., L. C. Lee, and K. Heki, Preseismic TEC changes for Tohoku-Oki earthquake:
5 Comparisons between simulations and observations. *Terr. Atmos. Ocean. Sci.*, 26, 63-72, doi:
6 10.3319/TAO.2014.08.19.06(GRT), 2015.
7
- 8 Jin, S., Occhipinti, G., Jin, R., GNSS Ionospheric Seismology: Recent Observation Evidences and
9 Characteristics. *Earth-Science Reviews* 147. Elsevier B.V.: 54–64.
10 doi:10.1016/j.earscirev.2015.05.003, 2015.
11
- 12 Liu, J.Y., Chen, Y.I., Chuo, Y.J., Chen, C.S., A statistical investigation of pre- earthquake
13 ionospheric anomaly. *J. Geophys. Res.* 111, A05304. [http:// dx.doi.org/10.1029/2005JA011333](http://dx.doi.org/10.1029/2005JA011333),
14 2006.
15
- 16 Lovelock J. E., Gaia as seen through the atmosphere, *Atmospheric Environment* 6 (8): 579–580.
17 1972.
18
- 19 Mancini, F., Galeandro, A., De Giglio, M., Barbarella, M., Assessing Ionospheric Activity by Long
20 Time Series of GNSS Signals: The Search of Possible Connection with Seismicity. *Physics and*
21 *Chemistry of The Earth* 16. Elsevier Ltd: 12002. doi:10.1016/j.pce.2014.10.005, 2014.
22
- 23 Martinelli, G., Solecki, A.T., Tchorz-Trzeciakiewicz, D.E., Piekarz, M., Grudzinska, K.K.,
24 Laboratory Measurements on Radon Exposure Effects on Local Environmental Temperature:
25 Implications for Satellite TIR Measurements. *Physics and Chemistry of the Earth, Parts A/B/C*,
26 April. doi:10.1016/j.pce.2015.03.007, 2015.
27
- 28 Masci, F, Thomas, J.N., Villani, F., Secan, JA., Rivera, N., On the Onset of Ionospheric Precursors
29 40 Min before Strong Earthquakes. *Journal of Geophysical Research: Space Physics*.
30 doi:10.1002/2014JA020822, 2015.
31
- 32 Meyers R. A., *Extreme environmental events*. Springer, New York, p 1250, 2009.
33



- 1 Mignan A., The Stress Accumulation Model: Accelerating Moment Release and Seismic Hazard,
2 *Adv. In Geophysics*, 49, 67–201, 2008.
3
- 4 Nanjo K.Z., Rundle, J.B., Holliday. J.R., Turcotte, D.L., Pattern Informatics and its application for
5 optimal forecasting of large earthquakes in Japan, *Pure app. Geophys.*, 163, 2417-2432, 2005.
6
- 7 Nott J., *Extreme events: a physical reconstruction and risk assessment*. Cambridge University Press,
8 Cambridge, p 297, 2006.
9
- 10 Ondoh, T., Anomalous sporadic-E layers observed before M 7.2 Hyogo-ken Nanbu earthquake;
11 Terrestrial gas emanation model, *Adv. Polar Upper Atmos. Res.*, 17, 96-108, 2003.
12
- 13 Ondoh, T., Hayakawa, M., Synthetic study of precursory phenomena of the M7.2 Hyogo-ken
14 Nanbu earthquake, *Phys. Chem. Earth*, 31, 378-388, 2006.
15
- 16 Ouzounov, D., Pulinets, S., Hattori, K., Kafatos, M., Taylor., P., Atmospheric Signals Associated
17 with Major Earthquakes. *A Multi-Sensor Approach*, Chapter 9, no. March: 1–23.
18 <http://hdl.handle.net/2060/20110012856>, 2011.
19
- 20 Peduzzi P., Is climate change increasing the frequency of hazardous events?, *Environment &*
21 *Poverty Times*, n.3, 7, 2005.
22
- 23 Perrone, L., Korsunova, L., Mikhailov, A., Ionospheric precursors for crustal earthquakes in Italy,
24 *Ann. Geophysicae*, 28, 941-950, 2010.
25
- 26 Piša, D., F. Němec, O. Santolik, M. Parrot, and M. Rycroft, Additional attenuation of natural VLF
27 electromagnetic waves observed by the DEMETER spacecraft resulting from preseismic activity, *J.*
28 *Geophys. Res. Space Physics*, 118, doi:10.1002/jgra.50469, 2013.
29
- 30 Piscini A., De Santis A., Marchetti D. and Cianchini G., A multi-parametric climatological
31 approach to study the 2016 Amatrice-Norcia (Central Italy) earthquake preparatory phase, *Pure*
32 *appl. Geophys.*, in press, 2017.
33



- 1 Piroddi, L., Ranieri, G., Freund, F., Trogu, A., Geology, Tectonics and Topography Underlined by
2 L'Aquila Earthquake TIR Precursors. *Geophysical Journal International* 197 (3): 1532–36.
3 doi:10.1093/gji/ggu123, 2014.
4
- 5 Pulinet, S.A., Boyarchuk, K.A., *Ionospheric Precursors of Earthquakes*. Springer Verlag, 2004.
6
- 7 Pulinet, S.A., Ouzounov, D., Ciralo, L., Singh, R., Cervone, G., Leyva, A., Dunajicka, M.,
8 Karelin, A.V., Boyarchuk, K.A., Kotsarenko, A., Thermal, atmospheric and ionospheric anomalies
9 around the time of the Colima M7.8 earthquake of 21 January 2003. *Annales Geophysicae*,
10 European Geosciences Union (EGU), 24 (3), pp.835-849, 2006.
11
- 12 Pulinet, S.A., Ouzounov, D., Lithosphere–Atmosphere–Ionosphere Coupling (LAIC) model. An
13 unified concept for earthquake precursors validation. *J. Asian Earth Sci.* 41, 371-382, 2011.
14
- 15 Pulinet S.A., Ouzounov D.P., Karelin A.V., Davidenko D.V., Physical bases of the generation of
16 short-term earthquake precursors: a complex model of ionization-induced geophysical processes in
17 the Lithosphere-Atmosphere-Ionosphere-Magnetosphere System, *Geomagnetism & Aeronomy*, No.4,
18 522-539, 2015.
19
- 20 Qin, K., Wu, L.X., De Santis, A., Wang, H., Surface latent heat flux anomalies before the Ms 7.1
21 New Zealand earthquake 2010. *Chinese Sci. Bull.* 56 (31), 3273–3280, 2011.
22
- 23 Qin, K., Wu, L.X., De Santis, A., Cianchini, G., Preliminary analysis of surface temperature
24 anomalies that preceded the two major Emilia 2012 earthquakes (Italy). *Ann. Geophys.* 55 (4), 823–
25 828, 2012.
26
- 27 Rundle, J.B., Tiampo, K.F., Klein, W., Martins, J.S.S., Self-organization in leaky threshold
28 systems: The influence of near mean field dynamics and its implications for earthquakes,
29 neurobiology and forecasting, *Proc. Natl. Acad. Sci. U.S.A.*, 99, suppl. 1, 2514-2521, 2002.
30
- 31 Row, R.V., Acoustic-gravity waves in the upper atmosphere due to a nuclear detonation and an
32 earthquake. *J. Geoph. Res.* 72 (5), 1599–1610, 1967.
33
- 34 Ruzhin, Y., Nomicos, C., Radio VHF precursors of earthquakes. *Nat. Hazard* 40, 573–583, 2007.



- 1
- 2 Schneider, S. and Boston P., *The Gaia Hypothesis and Earth System Science*. University of Florida.
- 3 MIT Press, 1992.
- 4
- 5 Scholz C.H., The frequency-magnitude relation of microfracturing in rock and its relation to
- 6 earthquakes, *Bull. seismol. Soc. Am.*, 58, 399-415, 1968.
- 7
- 8 Scholz, C.H., *The Mechanics of Earthquake and Faulting*, vol. xxiv. Cambridge Univ. Press,
- 9 Cambridge/New York (471 pp.), 2002.
- 10
- 11 Schorlemmer, D., S. Wiemer, and M. Wyss, Variations in earthquake size distribution across
- 12 different stress regimes, *Nature*, 437, 539–542, 2005.
- 13
- 14 Schreiber, T. , Measuring Information Transfer, *Phys. Rev. Lett.*, 85, 2, 461-464, 2000.
- 15
- 16 Shebalin P., Keilis-Borok, V., Gabrielov A., Zaliapin I., Turcotte D., Short-term earthquake
- 17 prediction by reverse analysis of lithosphere dynamics, *Tectonophysics*, 413, 63 – 75, 2006.
- 18
- 19 Scoville, J., Heraud, J., Freund, F., Pre-Earthquake Magnetic Pulses. *Nat.Hazards Earth Syst. Sci.*,
- 20 15, 1873-1880, 2015.
- 21
- 22 Shannon, C. E., A mathematical theory of communication, *Bell Syst.Tech. J.* **27**, 379, 623, 1948.
- 23
- 24 Signanini P., De Santis A., Power-law frequency distribution of *H/V* spectral ratio of seismic
- 25 signals: evidence for a critical crust, *Earth Planets Space*, 64, 49-54, 2012.
- 26
- 27 Silina, A.S., Liperovskaya, E.V., Liperovsky, V.A., Meister, C.V. Ionospheric phenomena before
- 28 strong earthquakes, *Natural Hazards and Earth System Sciences*, 1, 113-118, 2001.
- 29
- 30 Skinner BJ, Porter SC., *The blue planet: an introduction to earth system science*. Wiley VCH, New
- 31 York, 1995.
- 32
- 33 Sobolev G.A., Huang Q. and Nagao T., Phases of earthquake's preparation and by chance test of
- 34 seismic quiescence anomaly, *J. Geodynamics*, 33, 4-5, 413-424, 2002.



- 1
- 2 Sorokin, V.M., Chmyrev, V.M., Yaschenko, A.K. , Electrodynamic model of the lower atmosphere
3 and the ionosphere coupling. *J. Atmos. Sol. Terr. Phys.* 63, 1681–1691, 2001.
- 4
- 5 Stanley, H. E., *Introduction to phase transitions and critical phenomena*. Oxford University
6 Press, New York, 1971
- 7
- 8 Takens F., Detecting strange attractors in turbulence, Proceedings “*Dynamical Systems and*
9 *Turbulence, Warwick 1980*”, Lecture Notes in Mathematics, Volume 898. ISBN 978-3-540-11171-
10 9. Springer-Verlag, 1981.
- 11
- 12 Thomas, J.N., Masci, F., and Love, J.J. , On a report that the 2012 M 6.0 earthquake in Italy was
13 predicted after seeing an unusual cloud formation, *Nat. Hazards Earth Syst. Sci.*, 15, 1061-1068,
14 doi:10.5194/nhess-15-1061-2015, 2015.
- 15
- 16 Tiampo, K. F., Rundle, J. B., Klein, W., Premonitory seismicity changes prior to the Parkfield and
17 Coalinga earthquakes in southern California, *Tectonophysics*, 413, 77–86, 2006.
- 18
- 19 Tramutoli, V., Robust satellite techniques (RST) for natural and environmental hazards monitoring
20 and mitigation: theory and applications. In: *Proceedings 2007 International Workshop on the*
21 *Analysis of Multi-temporal Remote Sensing Images*,
22 <http://dx.doi.org/10.1109/MULTITEMP.2007.4293057>, 2007.
- 23
- 24 Tramutoli, V. , Using RST approach and EOS-MODIS radiances for monitoring seismically active
25 regions: a study on the 6 April 2009 Abruzzo earthquake. *Nat. Hazards Earth Syst. Sci.* 10, 239–
26 249, 2010.
- 27
- 28 Tyupkin, Y. S., Di Giovambattista, R. , Correlation length as an indicator of critical point behavior
29 prior to a large earthquake, *Earth Planet. Sci. Lett.*, 230, 85 – 96, doi:10.1016/j.epsl.2004.10.037,
30 2005.
- 31
- 32 Ulam S. M. and von Neumann J., On the Combinations of Stochastic and Deterministic Processes,
33 *Bull. Amer. Math. Soc.* 53, 1120, 1947.
- 34



- 1 Utsu, T., Estimation of parameter values in the formula for the magnitude-frequency relation of
2 earthquake occurrence, *Zisin* 31, 367-382, 1978.
3
- 4 Wang, L.-W., Shen, X.-H., Zhang, Y., Yan, R., Preliminary proposal of scientific data verification in
5 CSES mission. *Earthquake Science* 28 (4): 303–310. doi: [dx.doi.org/10.1007/s11589-015-0131-2](https://doi.org/10.1007/s11589-015-0131-2),
6 2015.
7
- 8 Wu L.X., Zheng S., De Santis A., Qin K., Di Mauro R., Liu S.J. and Rainone M. L., Geosphere
9 Coupling and Hydrothermal Anomalies before the 2009 Mw 6.3 L'Aquila Earthquake in Italy,
10 *Nat. Hazards Earth Syst. Sci.*, 16, 1859-1880, doi:10.5194/nhess-2015-346, 2016.
11
- 12 Xie, T. and Weiyu, M., Possible Thermal Brightness Temperature Anomalies Associated with the
13 Lushan (China) MS7.0 Earthquake on 20 April 2013. *Earthquake Science* 28 (1): 37–47.
14 doi:10.1007/s11589-014-0106-8, 2015.
15
- 16 Xiong, Pan, Xuhui Shen, Xingfa Gu, Qingyan Meng, Yaxin Bi, Liming Zhao, Yanhua Zhao, Yan Li,
17 and Jianting Dong, Satellite Detection of IR Precursors Using Bi-Angular Advanced along-Track
18 Scanning Radiometer Data: A Case Study of Yushu Earthquake. *Earthquake Science* 28 (1): 25–36.
19 doi:10.1007/s11589-015-0111-6, 2015.
20
- 21 Xu, T., Hu, Y.L., Wang, F.F., Chen Z., Wu J., Is there any difference in local time variation in
22 ionospheric F2 layer disturbances between earthquake induced and Q- disturbances events?, *Ann.*
23 *Geophysicae*, 33, 687-695, 2015.
24
- 25 Zoller, G., Hainzl, S. A systematic spatiotemporal test of the critical point hypothesis for large
26 earthquakes. *Geophys. Res. Lett.*, 29, 1558, 2002.
27